

Central Electricity  
Generating Board

**Information Services**

Sudbury House,  
15 Newgate Street,  
London EC1A 7AU

1972  
C.E. Translation

6253

Archivexemplar

Methods and results of research on lightning on Mount San Salvatore 1963-1971

K.BERGER

Bull. ASE, Vol.63, No.24, pp. 1403-1422, (25 Nov. 1972)

Any illustrations in the original text are reproduced in this translation by an economical method. If greater definition is required, readers should refer to the original text, which is obtainable from appropriate libraries.

Methods and results of research on lightning on Mount San Salvatore 1963-1971

K. BERGER

Bull. ASE Vol. 63, No. 24, pp. 1403-1422, (25 Nov. 1972)

Abstract

This paper is a continuation of previous reports on research on lightning on Mount San Salvatore in 1945-1954 and 1955-1963 (Lightning Current Measurements) (Bib. 1), 1955 to 1965 (Photography) (Bib. 2) and first measurements in the field close to the lightning stroke (1968) (Bib. 3). The first chapter of the final report below discusses the equipment developed and used up to 1971 for measuring the lightning current and the field strength associated with lightning strokes. The second chapter is concerned with the evaluation of currents of 126 downward strokes to the measuring towers on the mountain. For this purpose, the oscillographically measured current curves of all downward strokes were converted to a linear time scale by a computer at the ORL Planning Institute of ETH and were reproduced in an "index of lightning currents". After this, based on detailed evaluation of all lightning-current oscillograms, there follows statistical representation on probability type graph paper of all characteristic data of lightning currents, such as the peak, current steepness, charge, energy impulse, duration of current and current intervals. Thirdly, the correlations of individual characteristic data are represented in graphs based on probability theory. Fourier frequency analysis is performed on two oscillogram traces.

Methods and results of research on lightning on Mount San Salvatore 1963-1971

K. BERGER

Bull. ASE Vol. 63, No. 24, pp. 1403-1422, (25 Nov. 1972)

This paper is a continuation of previous reports on research on lightning on Mount San Salvatore in 1945-1954 and 1955-1963 (Lightning Current Measurements) (Bib. 1), 1955 to 1965 (Photography) (Bib. 2) and first measurements in the field close to the lightning stroke (1968) (Bib. 3).

The first chapter of the final report below discusses the equipment developed and used up to 1971 for measuring the lightning current and the field strength associated with lightning strokes.

The second chapter is concerned with the evaluation of currents of 126 downward strokes to the measuring towers on the mountain. For this purpose, the oscillographically measured current curves of all downward strokes were converted to a linear time scale by a computer at the ORL Planning Institute of ETH and were reproduced in an "index of lightning currents". After this, based on detailed evaluation of all lightning-current oscillograms, there follows statistical representation on probability type graph paper of all characteristic data of lightning currents, such as the peak, current steepness, charge, energy impulse, duration of current and current intervals. Thirdly, the correlations of individual characteristic data are represented in graphs based on probability theory. Fourier frequency analysis is performed on two oscillogram traces.

The variation and magnitude of the electric fields prior to and during lightning striking the mountain and the simultaneous field jumps in the vicinity of the mountain will be described in a second paper, as will the conclusions to be drawn from the whole body of results concerning the protection of both persons and objects against lightning.

1. Description of measuring instruments used in research on lightning 1963-1971

1.1 Instruments for measuring the lightning current

Subject to minor modifications, the same instruments were used as in the previous period, 1955-1963 (Bib. 1). Figs. 1 and 2 show the system of current measurement, Fig. 1 illustrating equipment at the top of every tower, and Fig. 2 the equipment in the Faraday cage of the measuring chamber in the so-called "Antico Albergo". For the sake of convenience only the instruments per tower have been indicated. The explanation of the diagrams will be found in the detailed captions. For both towers together, there are available for current measurement 8 measuring loops of the oscillograph with loops (SO) and 2 dual-beam

cathode-ray oscillograph tubes (KO). Two further single-beam KO were used to measure the field variation in Tower 1 and to record the time base. These six variables were recorded by the KO on a photo-sensitive chart with a width of 12 cm and a length of 1 m, in such a way that using an additional rapid time base, it was possible to record even rapid changes in lightning current. The SO in turn recorded the long-duration lightning current components and, with the assistance of a storage circuit, the positive and negative peaks of the lightning current impulse.

During the period under review two new ranges were introduced in the field-strength oscillograms for the measurement of small pre-discharges of the lightning which occurred prior to the triggering of the lightning oscillograms, i.e. prior to the shreshold of about 7 A lightning current (response of the gap FH in Fig. 1). The first range added included currents up to 7 mA, the second included currents up to 1 A. Since these currents were present prior to the coming into action of the gap FH, i.e. prior to the triggering of the lightning-current oscillograms, they had to be stored, in the same way as the oscillograms of field variation, prior to the lightning stroke. Section 2 describes how this was done. The recording of these small currents on the same chart as for the field variation allowed exact timing of pre-discharge and field.

## 1.2 Instruments for measuring field variation in the event of a lightning flash

A first field mill of classical design was installed in Tower 1 in 1967 and operated on the south eastern face of the tower at a height of about 18 m above ground level (Fig. 3). It consisted of 24 segments on a plate which rotated at just under 3,000 rpm or about 50 rps (synchronous rpm 3,000/min). From this we obtained a limit frequency of about 1,200/s. This field mill was described in CIGRE Report No. 33-03, 1968 (Bib. 3) which also reported a few first results. Since then it has been performing satisfactorily but it has the disadvantage of producing a loud noise like an air raid siren which greatly restricts its use in built-up areas. For field measurements in the vicinity of Lugano it became necessary to design a device which would avoid this disadvantage and, if possible, have a limit frequency higher than 1,200/s.

With financial support from the Swiss National Fund for scientific Research, a new type of field mill based on a suggestion by E. Vogelsanger was designed the principle of which is briefly described in Figs. 4 and 5. A more detailed description will be published elsewhere.

Fig. 4 represents the charges  $Q$  of the measuring plates of two field mills the measuring segments of which are offset by half a cycle,  $T/2$ . Consequently, adding up of the charges of the measuring discs with the rotation time  $T$  (of 2 field mills displaced by  $T/2$ ) produces a constant sum  $Q_1 + Q_2$ . The total charge of the exposed surface will therefore at all times be dependent solely on the electrical field strength  $E$  and not on its variation with time.

$$Q = Q_1 + Q_2 = \text{Const.} \times E$$

This is valid for any even number  $n$  of field mill segments of an individual measuring plate, displaced by  $T/2n$ , when all even or uneven segments are exposed to the atmospheric field simultaneously. In principle the sum of exposed surfaces remains constant.

Theoretically such field mills would therefore be suitable for recording any desired frequency range from zero to infinity. In practice all these field

mills suffer from a defect which is fundamentally the same as that of field measurements on aerials: the leakage currents flowing through the high insulation of aerial or measuring plate cause the measuring plate to acquire a mean voltage to earth in the event of a prolonged constant atmospheric field strength, because this alone will on average prevent discharge current from flowing. In other words, the zero line of the field oscillograms is displaced.

This fundamental problem can be overcome in field mills by connecting every measuring segment momentarily to earth at the points of full screening (Points T, 2T or 0.5 T, 1.5 T ..., Fig. 4). Since this short circuiting to earth requires a certain time even when high speed relays are used, this amount of time must be taken into account when designing the instrument by providing a third time step within the time T for segment earthing.

Fig. 5 illustrates this idea. The period T is divided into 3 parts T/3. Apart from the rise (1st third  $Q_1$ ) and the falling off (2nd third  $Q_1$ ) provision is made for a third part of the time T during which the measuring disc is completely screened and the voltage should be zero. In theory this zero voltage is enforced by mechanical relays (reed relays) because otherwise the insufficient insulation of the plates would cause gradual deviation. Fig. 6 shows the new field mill in the operating condition and when opened.

Fig. 7 shows the total layout of the 5 existing field mills for 3,000 rpm which are constructed on this principle. The following components are mounted on a joint axis:

the static measuring plate MP with 6 segments each of  $60^\circ$ ,

the rotating screening plate B the aperture of which corresponds exactly to 2 opposed measuring segments

the rotating permanent magnet NS

the fixed ring R with 6 reed relays as switches which are operated by the magnet NS

the bi-polar asynchronous motor AM,

a heating coil H to prevent formation of dew.

Two opposed segments of the measuring plate MP are joined, as are the two associated reed relays on the ring R. The electrostatic charges of the measuring segments MP are passed to the capacitors CL which are intended to compensate the fluctuations of measuring plate capacity. The position of the ring R with the switching relays is adjusted in relation to the screening plate B so that it corresponds to that shown in Fig. 5, i.e. those segments are earthed by the reed relays which are completely located under the solid part of B. The asynchronous motor revolves at 3,000 rpm or 50/s. The cycle T consequently is about  $1/50 \text{ s} \approx 10 \text{ ms}$ , the duration of full screening ("zero time")  $T/3 \approx 3.3 \text{ ms}$ . Within this period every measuring plate must first be earthed and then insulated from earth. The charges or voltages of the 6 measuring segments are collected in the Philbrick Nexus amplifier model Q 103 U 5801 ( $\Sigma$ ), are amplified and passed as a sum via the potentiometer T to the transducer W-V for transmission to San Salvatore (Fig. 8).

The other instruments shown in Fig. 7 are used for calibrating the field mill with positive and negative calibration voltages by means of the parallel relays

PR and the calibration relays CR<sub>1</sub> and CR<sub>2</sub>, and for recording the oscillogram zero line by earthing the measuring sectors by means of the relay ER. All the relays are remotely controlled from San Salvatore via the point FE.

The transmission of data collected by the field mills to San Salvatore and the associated oscillographs in the control centre at the "church" are shown in Fig. 8. A description of the arrangement of the new field mills at the four measuring points Agra - Gemmo - Pugerna - San Salvatore 2 will be given in the report of the results of open-air measurement which will also contain photographs illustrating the installation of field mills. Transmission of variable DC at the output of the field mills to the measuring instrument on San Salvatore is effected by modulation of a carrier frequency of 13.5 kHz via the post office cables of the Lugano area. Non-coil-loaded cables only could be used for this purpose which restricted the choice of measuring points in a southerly direction. The modulated signals were stored on a strip-chart recorder made by the P. Klein Company at Tettwang on a 7-track magnetic tape, and were erased before the tape had completed its cycle which took 5 s. The demodulated signals were recorded by the oscillograph "Osz", Fig. 8, as soon as the lamp of the latter was switched on as the result of lightning striking the measuring towers. This was done by the trigger T (Fig. 2) via K4 to the control instrument St, Fig. 8. The damping of transmission corresponded to the lengths of cable given in Table I. It remained within acceptable limits for all 3 external measuring points, the measuring point at Agra approaching the limit of permissible damping. The maximum permissible frequency of field measurements was about 4 kHz due mainly to the measuring loops of the oscillograph, and also to the carrier frequency of 13.5 kHz which allowed transmission of measuring frequencies only slightly higher than 4 kHz.

The "new" field mills were all remotely controlled (FE, Fig. 7 and St, Fig. 8). Control included switching on and switching off the motor selecting a channel for greater or lesser sensitivity (potentiometer T with change-over switch, Fig. 7), parallel connection of plates for calibration (relays PR and CR) and earthing of the plates (relay ER) for recording the zero line of the oscillograms. Calibration was done with 2 direct voltages taken from the 50 Hz voltage with 2 different amplitudes of +6V and -4V. This allowed the polarity of the voltages measured to be checked in the oscillogram. Remote control was done by 3 fixed frequencies with filters. Field strengths were recorded on the oscillograph charts for about 1 s prior to and 1 s after the lightning had struck, at a chart feed rate of about 1 m/s or 1 mm/ms.

Obviously the field curves can also be recorded for any lightning other than that striking Mount San Salvatore. Because of the storage for 5 s there was sufficient time to operate the push button for oscillograph paper feed and for the lamp to allow the field to be recorded oscillographically prior to, during and after the occurrence of lightning.

## 2. Recording of thunderstorms and lightning

### 2.1 Number of thunderstorm days and recording of thunderstorms

As in the case of the previous reports, Table II records the number of thunderstorm days observed on San Salvatore per month and year and the duration of observation in the various years 1963-1971. A thunderstorm day (isoceraunic level) is defined as a day (24 hours) on which thunder was heard at least once at the point of observation. Fig. 9 presents Table II in graph form.

Evidently the figures for the top of San Salvatore are higher than those counted for example in the city of Lugano, since the noise level in the town was so high that it was impossible to hear distant thunder there, but not on the mountain. Nowadays, meteorologists would like to supplement the counting of thunderstorm days by more information about the thunderstorm activity. This can be done by means of "lightning flash counters", which count the number of lightning flashes in an area corresponding approximately to the audibility range of thunder (about 20 km radius). Such counters have been distributed by the "lightning flash counters" working group of CIGRE for years, and world-wide data have been collected on the relative frequency of lightning flashes in various parts of the world (Bib. 4).

Lightning flash counters of various kinds were used for a time on San Salvatore. However, the topographic conditions on the mountain made comparison with standard metering in the plain impossible, and we shall therefore refrain from reporting these data. For recording thunderstorms, the continuous recording of glow discharge and displacement currents of the lightning aeri-als on Towers 1 and 2 (instrument G in Fig. 2) has proved itself on San Salvatore. The very simple instrument which has been described previously utilises, for counting lightning flashes, the field strength impulses the lightning flash causes in its vicinity. As in the case of the CIGRE lightning flash counter the metering range cannot be sharply defined, because strong lightning flashes can be detected at greater distances than weak lightning flashes. Continuous recording of the number of lightning flashes or field jumps allowed better assessment to be made of the possibilities of issuing thunderstorm warnings to work places subjected to lightning hazards than measurement of field strength. The results of this investigation cannot be discussed in detail here.

## 2.2 Number of oscillograms recorded during the period under review

Table III provides information about the total number of oscillograms recorded and evaluated in the years 1963-1971. In all, about 1,000 determinations were made of lightning currents, classified by polarity and direction of propagation. Some of these lightnings flashes are multiple flashes, viz. about 240. Table IV indicates their distribution over the various years. The two tables show that the scatter of determinations and of the number of lightning flashes over the years was within 1:3 or 1:4. The "oscillogram-rich" years of San Salvatore do not coincide with the thunderstorm - rich years in Lugano and its vicinity because in long and violent thunderstorms the mountain frequently fails to be struck by lightning whereas in weak thunderstorms the mountain may be struck repeatedly.

A further classification of lightning flashes, by the number of strokes per flash, is given in Table V.

Another way of distinguishing between lightning flashes follows from their origin i.e. from their direction of propagation. It is possible in most cases to decide from the temporal variation of the current in the lightning current oscillograms whether a downward stroke or an upward stroke is involved. The terms are defined in the section that follows.

Table VI shows the number of downward strokes in the years 1963-1971 and the frequency of positive and negative single flashes. It may be assumed that these downward strokes which form in the clouds and propagate from there to the ground occur in the same manner on mountains and in the plains so that they are of interest for all topographical locations whether it be a mountain, a cliff, a plain or a lake. In contrast with this, upward strokes only form on high

structures in particular towers, or masts, on hills or mountain tops. Table VI shows that of a total of 1,000 lightning flashes striking the two measuring towers on San Salvatore only 126 came from downward strokes, i.e. only 13%. Scatter over the various years was even greater, i.e. up to about 1:6.

### 3. The lightning-current index

The current oscillograms of all downward strokes were converted to a linear timescale with the assistance of the computer of the Institute for ORL-Planning of ETH, the timescale as a rule covering the interval of 150  $\mu$ s, and, in the case of long-duration flashes, 1500  $\mu$ s. In this way a total of 116 downward strokes were recorded with their consecutive strokes and their variation with time in a "lightning-current index". Fig. 10 provides a few examples taken from this index (the index can be obtained at cost from the author). The strokes of multiple flashes are marked a-b-c. Underneath every oscillogram will be found the computer number, the digits of which indicate minute, hour, day, month, year, number of oscillogram and tower number (T1 or T2).

For evaluating the oscillograms and for describing the lightning flash it is necessary to define terms. The terms listed below closely follow and supplement English usage.

### 4. Terminology of lightning

#### 4.1 General terms

- (a) The lightning flash, or in short, "flash" is the totality of an atmospheric discharge consisting of one or several lightning strokes (Schonland's definition)
- (b) The lightning stroke, in short, "stroke", is a partial discharge which is initiated by a leader stroke (Schonland's definition)
- (c) The leader is the low-light and low-current pre-discharge which in propagating opens the lightning channel (Schonland).
- (d) The lightning channel is the conducting path of the lightning current
- (e) The return stroke or main stroke is the luminous high current discharge which occurs when the leader comes into contact with the ground (Schonland).
- (f) The downward stroke is a stroke the leader of which propagates from the cloud towards the ground.
- (g) The upward stroke is a stroke the leader of which starts on the ground or from an earthed conductor and propagates towards the clouds.
- (h) The single-stroke flash, or, in short, "single flash", is lightning consisting of a single stroke
- (i) The multiple-stroke flash, or in short, "multiple flash", is a flash consisting of several lightning strokes.

- (k) The consecutive or following stroke is a stroke which follows the first lightning stroke or a consecutive stroke.
- (l) The duration of a flash is the total duration of a flash as determined electrically or photographically by a defined method
- (m) The duration of a stroke is the duration of a lightning stroke (leader plus return stroke)
- (n) The stroke interval is the time that elapses between the beginning of two lightning strokes (Kitagawa)
- (o) The connecting streamer is the discharge from earthed objects or from the ground that propagates towards the leader of a downward stroke.

#### 4.2 Special terms to describe the lightning current

- (a) Lightning current is the peak of the current measured with the assistance of a shunt at the top of the measuring tower and of a measuring cable oscillographically on the ground
- (b) The impulse current is the peak of the short-duration, high component of the lightning current
- (c) The continuing current is the linear mean value of the long-duration component of the lightning current
- (d) The front is the ascending part of the lightning current curve.
- (e) The tail is the descending part of the lightning current curve
- (f) The front duration or rise-time of a lightning current is the time that elapses between the beginning and the peak of the lightning current. The beginning is understood to mean the moment of time when the impulse current reaches 2kA. If the current curve has several peaks, the first peak is selected
- (g) Current steepness is the maximum current variation ( $di/dt$ ) during the lightning current front in lightning strokes.
- (h) The electric charge or current impulse of a flash or stroke is the time integral of the lightning current. It can be calculated for the impulse current and the continuing current of flashes or strokes
- (i) The current-square impulse is the integral  $\int i^2 dt$  for the duration of a lightning stroke. It can be calculated for the impulse current and the continuing current of a flash or stroke.
- (k) The zero-current interval is the duration of the zero-current interval between two lightning strokes as determined on the ground.

## 5. The distinction between upward and downward strokes in the current oscillograms

In the present report the difference between downward and upward strokes is determined from the curve variation of the lightning current oscillograms because this method can be used even in daylight (lightning photography, in particular photography of a propagating lightning channel, fails in daylight.)

In the large majority of cases differentiation based on the oscillograms is unambiguous because in the case of the upward stroke the lightning current starts with a gradually increasing "continuous current" of an order of magnitude of 50-500 A whereas the downward stroke begins with a steep current impulse i.e. with current steepness of the order of magnitude of kA/ $\mu$ s.

Uncertainty arises in some circumstances as a result of the connecting streamer of downward strokes when this connecting streamer is very long and consequently lasts long. This manifests itself in a current curve which at first does not differ greatly from that of an upward stroke. From this latter it differs only in that after a relatively long period, i.e. not just some 50  $\mu$ s in accordance with the duration at that stage of the flash, but after about 1 ms or more, a high impulse current occurs with the corresponding steep front of a downward stroke. Such cases were reported in the previous paper in 1966 (Bib. 2).

The terms, upward and downward stroke are no longer unambiguous in that an upward stroke as it were fetches down a downward stroke from the clouds. In the present paper the line between them has been drawn by speaking of a downward stroke in spite of the long connecting streamer if the impulse charge is considerably greater than the charge stored in the connecting streamer. These two charges can be evaluated from the oscillograms.

The "fetching down of a lightning stroke" by a long connecting streamer which at first sight appears improbable no longer looks anomalous in view of new measurements of field distribution prior to and during the lightning stroke, which show that the lightning flash often is only a modest part of a much more comprehensive event in the clouds, which in many cases precedes the flash.

## 6. Statistical evaluation of lightning currents

It proved possible using the ETH computer to calculate in the first instance the current oscillograms of all downward strokes of the period 1968-1971 in statistical form. This evaluation applies to the representation of the data in Table VII on probability graph paper with a log scale on the abscissa. Of the 31 frequency curves calculated, 10 examples are reproduced below, Figs. 11 - 20 (the graphs, Table VII, can be obtained at cost from the author).

The curves show the regression line calculated by the computer, on assumption of log-normal frequency distribution and least squares deviation, and, in some cases, the 95% confidence limit.

The space available does not permit us to discuss in detail the interesting features of the diagrams; only a few general observations can be made:

6.1 Whereas, in the case of some data, for example, the peak of all strokes (i of all strokes), Fig. 14, we can speak of log-normal distribution as a good approximation, this cannot be done with other data, such as the steepness of the first strokes (Fig. 19).

6.2 About 10% of all negative stroke currents had a steepness of 50 kA/ $\mu$ s or higher. Figures of 60 kA/ $\mu$ s or higher must be considered with caution because the accuracy of measurement of the existing instruments was no longer definitely sufficient. Insofar as there is practical interest in these steepest currents, complementary determinations would be desirable. It must however be pointed out that the steepest tangent to the current curve was used for evaluation. This only occurs in the case of the first stroke just before the current peak and is therefore of fundamental importance in lightning protection (Bib. 5). As we know, a steep slope occurs in all consecutive strokes, the current peaks of which with very few exceptions are however smaller than in the case of the first stroke. This problem of correlation between current and steepness will be discussed in Chapter 7 (Correlations).

6.3 There is a similar reservation concerning front durations: with the existing instruments it proved impossible to measure front durations of less than 0.5  $\mu$ s with accuracy at high peak currents, or large deflections in the oscillogram, so that complementary measurements may again be necessary. The short front durations invariably occurred in the case of consecutive strokes.

6.4 Insofar as the frequency corresponded to log normal distribution, the occurrence of rare extreme values can be estimated. It would be expected that

about 5% of all positive downward strokes carry more than 300 kA and

about 0.2% of all positive and negative downward strokes carry more than 300 kA

or, in relation to the current square impulse which corresponds to the energy impulse in 1  $\Omega$  that

about 10% of all positive downward strokes carry more than  $10^7$  A<sup>2</sup>s and

about 0.5% of all positive and negative downward strokes carry more than  $10^7$  A<sup>2</sup>s.

The highest lightning current measured during the period under review and during the total period of detailed determinations on Mount. San Salvatore (1964 to 1971) amounted to about 270 kA. Of the total of lightning currents measured since 1946 i.e. 1026 + 379 + 272, this corresponds to a probability of about 0.6 per thousand, and of the total number of downward strokes measured during 1963 to 1971, i.e. 126, it amounts to about 8 per thousand, whereas, of the 28 positive downward strokes measured, it amounts to about 4%.

## 7. Correlation of lightning current characteristics

### 7.1 Object and reproduction

In applying the results of research on lightning to the problems of protection against lightning, the question frequently arises as to how frequently unfavourably high levels of different lightning current characteristics coincide. For example the voltage of a lightning conductor for a building in relation to the surrounding earth comprises an inductive voltage drop along the lightning conductor  $L \times di/dt$  and an ohmic proportion at the earth  $R_e i$  These

two can be of the same order of magnitude; the voltage attains a maximum when, the maximum current coincides with the maximum current steepness  $di/dt$ , or in other words when there is a definite correlation of the two. A similar problem arises in the case of surge diverters their loading becomes a maximum when, with the same lightning stroke having the highest  $i$  values, the highest  $Q$  values or the longest current duration also occur.

Testing the statistical correlation of any of two characteristic lightning factors can best be done by entering all data in a co-ordinate system, the first being used as abscissa and the second as ordinate. From the cluster of data it will be possible to estimate whether a correlation is probable. On the other hand the computer allows calculation of the regression of two factors in that for example investigation is made of whether regression can be observed with a given degree of probability. One such investigation was carried out on the computer of the ORL Planning Institute of ETH Zurich.

From digital data storage the computer determined the correlations of lightning current characteristics and recorded regression curves.

Table VIII lists 27 graphs of possible correlations, in particular between the current peaks and other characteristics such as charge, steepness, energy impulse and duration of the lightning current.  $n$  indicates the number of determinations, of which 8 examples are given below. Figs. 21-28. (The graphs, Table VIII, can be obtained from the author at cost). Distinct correlations exist between  $i$  and the impulse charge  $Q$  or  $\int idt$  and between  $i$  and  $\int i^2dt$ , if only the current impulse and not the long-duration current component is taken into account. A few theoretical observations on the problem of the so called "protected space" of lightning conductors follow.

## 7.2 Problem of the "protected space" of a lightning conductor

The firm connection between the peak current and the impulse current of a stroke provides the basis for the only still tenable theory of the so-called "protected space" provided by lightning conductors, within which no lightning should strike. An account of this theory was published by R.M. Golde in 1961 (Bib. 6, 7). Indeed, theoretically, at a certain charge distribution along a leader of given length (which is imagined to be unramified) the potential of the leader head prior to the lightning stroke should be proportional both to the peak lightning current and to the charge stored in the leader. The scatter of the data for the correlation  $i$  (impulse) and  $Q$  (impulse) may be due on the one hand to the length of the flash, or, on the other, to the not-always-uniform charge distribution of the leader, in other words, in practice, above all to the presence of channel ramification ('lightning branching') which increases the impulse charge of the first lightning current impulse but not its peak current. The curves, Figs. 25 to 28 show that there exists an approximate proportionality between impulse charge and peak current of the lightning-current impulse, and also a difference between positive and negative first strokes.

Concerning the question of the space protected from lightning there remains in addition the open question as to the correlation between the very high potential of the leader head and the striking distance. If there is a definite correlation, it is possible to calculate a protected space from the above-mentioned established correlation between  $i$  and the impulse charge  $Q$ . However if, at these high voltages, there is no longer a definite correlation between the strike distance and measurement, the same uncertainty will also affect the so-called protected space. Tests carried out with so-called 'switching surges'

of more than 2 MV with front durations of several 100 to 1,000  $\mu$ s in large high voltage laboratories showed that there was no longer a definite correlation between positive rod and point electrodes (Bib. 8). Since, in the downward stroke, the leader head must be considered as the tip, this uncertainty exists in particular in the rare case of high current and charge intensity lightning flashes from positive clouds. In spite of the evidence in support of the correlation between  $i$  and  $Q$  (impulse) the question as to the possibility of a defined protected space must therefore be assessed sceptically in theory.

#### 8. Spectrum analysis of the impulse components of lightning currents

Digital storage of the curves of impulse currents of downward strokes allows a frequency analysis to be made. Because the time available since storage began was limited only a few examples of current curves have been analysed, selecting either a lightning current recorded at the usual time interval of 150  $\mu$ s, or a long-duration lightning current with just over 1,000  $\mu$ s duration. Analysis was done by the classical method of Fourier analysis of digital time series at the Computer Centre of ETH Zurich. Fig. 29 shows the results of one such analysis for two extreme forms of current.

The frequency components in the range of about  $10^3$  to  $10^5$  Hz in negative, and about 300 -  $10^5$  Hz in positive lightning currents are reduced from about 95% to a few per cent. Now we know that in the case of atmospherics, i.e. in the case of electrical fields caused by lightning at distances of hundreds or thousands of kilometres from the flash higher frequencies are predominantly detected. This phenomenon must in the first instance be attributed to the fact that within the radiation field of a dipole the higher frequencies are transmitted with less damping than the low frequencies, so that the former tend to predominate increasingly with increasing distance. On the other hand, field measurements in the vicinity of the flash also show frequency fractions of MHz with relatively small amplitudes. These must probably be attributed to the fine ramifications of the flash in the clouds, which are not apparent in the current distribution on the ground.

Results of field measurements in the immediate vicinity of the lightning stroke and in the area surrounding it will be reported in a second paper, to be published in one of the next issues of Bull ASE.

We wish to express our gratitude to the Swiss National Fund for scientific research which made the tests described possible and to H. Kröniger, Pretoria who was responsible for statistical evaluation and oscillogram linerarisation, assisted by various institutes of ETH and staff of FKH.

Table 1: Transmission cables from the field mill outstations to Mount San Salvatore

Agra point to point distance 3.3 km	0.97 km dia. = 0.4 mm Cu
	2.76 km dia. = 0.6 mm Cu
	3.46 km dia. = 0.8 mm Cu
	4.13 km dia. = 1.0 mm Cu
	<u>11.32 km</u>
Gemmo point to point distance 3.45 km	1.30 km dia. = 0.6 mm Cu
	0.19 km dia. = 0.8 mm Cu
	4.13 km dia. = 1.0 mm Cu
	<u>5.62 km</u>
Pugerna point to point distance 2.5 km	4.53 km dia. = 0.6 mm Cu
	4.13 km dia. = 1.0 mm Cu
	<u>8.66 km</u>

Table II: Number of thunderstorm days (isoceraunic level) according to observations on Mount San Salvatore 1963 - 1971

Year	Curve Fig.9	Month March	Month April	Month May	Month June	Month July	Month Aug.	Month Sept.	Month Oct.	Month Nov.	Total	Period under observation
1963	1	1	12	14	16	17	13	8	2	-	83	18.3 to 21.10
1964	2	1	8	8	15	13	8	6	3	-	62	23.3 to 4.10
1965	3	-	4	10	11	14	11	10	0	-	60	15.4 to 4.10
1966	4	1	8	13	14	12	12	5	3	-	68	17.3 to 21.10
1967	5	2	7	10	12	17	11	8	4	1	72	10.3 to 28.11
1968	6	2	7	11	14	10	14	9	4	4	75	26.3 to 26.11
1969	7	3	1	13	9	17	18	13	0	3	77	1.3 to 21.11
1970	8	1	7	7	15	9	11	9	1	-	60	6.3 to 2.11
1971	9	1	2	15	16	13	17	3	0	1	68	25.3 to 24.11
Average 1963-1971	10	1.3	6.2	11.2	13.6	13.6	12.8	7.9	1.9	1	69.5	

Table III: Total number of oscillograms recorded 1963-1971

Year	↓ -	↑ -	↓ +	↑ +	Bipolar		Total
					↓	↑	
1963	22	83	3	5	1	4	118
1964	6	37	1	6	0	6	56
1965	3	91	1	15	0	8	118
1966	6	120	5	19	3	7	160
1967	12	90	9	26	0	13	150
1968	2	85	4	5	0	3	99
1969	3	38	2	6	1	2	52
1970	32	68	0	2	0	6	108
1971	20	120	2	18	0	5	165
1963 to 1971	106	732	27	102	5	54	1026

Table IV: Number of oscillograms of multiple flashes 1963 - 1971

Year	↓ -	↑ -	↓ +	↑ +	Bipolar		Total
					↓	↑	
1963	11	14	0	0	0	1	26
1964	3	8	0	0	0	3	14
1965	1	24	0	0	0	4	29
1966	1	27	0	2	1	2	33
1967	3	24	0	1	0	8	36
1968	1	20	0	1	0	1	23
1969	1	6	0	0	0	2	9
1970	13	15	0	0	0	4	32
1971	9	26	1	0	0	3	39
1963 to 1971	43	164	1	4	1	28	241

Table V: Number of lightning flashes with the number of strokes indicated below 1 - < 10 1963 - 1971

Year	Number of oscillograms evaluated	Number of strokes in the flashes										
		1	2	3	4	5	6	7	8	9	10	> 10
1963	118	92	7	5	3	4	2	1	-	-	1	3
1964	56	42	6	2	3	1	2	-	-	-	-	-
1965	117	89	9	7	1	4	-	-	-	-	1	6
1966	159	127	10	7	3	3	1	1	3	1	-	3
1967	150	114	12	4	2	5	3	3	1	1	-	5
1968	101	76	9	5	1	3	1	1	1	1	-	3
1969	52	43	3	3	-	-	-	1	-	-	1	1
1970	108	75	8	7	6	3	1	1	1	2	2	2
1971	165	126	15	9	1	1	4	2	1	-	1	5
1963 to 1971	1026	784	79	49	20	24	14	10	7	5	6	28

Table VI: Number of single flashes in downward strokes 1963 - 1971

Year	Number of downward strokes	Number of single flashes	Single flashes	
			Positive	Negative
1963	24	15	4	11
1964	7	4	1	3
1965	4	3	1	2
1966	13	12	7	5
1967	17	8	0	8
1968	5	4	2	2
1969	6	5	3	2
1970	30	19	0	19
1971	20	12	1	11
1963 to 1971	126	82	19	63

Table VII: Statistical representation of some lightning variables

1.	Peak of lightning current	all strokes	n = 262
2.		all positive strokes	n = 28
3.		all negative strokes	n = 236
4.		all first strokes	n = 126
5.	Charge of lightning current	in 119 lightning flashes	
6.		in 27 positive flashes	
7.		in 88 negative flashes	
8.		in 241 strokes	
9.		in 26 positive strokes	
10.		in 215 negative strokes	
11.		for 117 first strokes	
12.	Charge of impulse component of lightning current	in 232 strokes	
13.		in 25 positive strokes	
14.		in 207 negative strokes	
15.		in 113 first strokes	
16.	Steepness of lightning current	in 235 strokes	
17.		in 21 positive strokes	
18.		in 212 negative strokes	
19.		in 111 first strokes	
20.	Current square impulse of lightning current	206 strokes	
21.		27 positive strokes	
22.		179 negative strokes	
23.		115 first strokes	
24.	Duration of flash	in 118 lightning flashes	
25.		in 26 positive flashes	
26.		in 93 negative flashes	
27.	Front duration of lightning current	in 226 strokes	
28.		in 19 positive strokes	
29.		in 207 negative strokes	
30.		in 106 first strokes	
31.	Time interval	in 133 stroke intervals	

Table VIII: Reproduction of correlation of the factors listed below

1	The current peak, over total charge of a lightning flash	All lightning flashes	n = 119
2.		Positive flashes	n = 26
3.		Negative flashes	n = 93
4.	Current peak over impulse charge of a stroke	First strokes	n = 113
5a.		Positive first strokes (log scale)	n = 24
5b.		Positive first strokes (linear scale)	n = 24
6a.		Negative first strokes (log scale)	n = 89
6b.		Negative first strokes (linear scale)	n = 89
7.		Consecutive flashes	n = 118
8.	Current peak over current steepness	First strokes	n = 111
9.		Positive first strokes	n = 20
10.		Negative first strokes	n = 91
11.		Consecutive strokes	n = 123
12.	Current peak over current square impulse	First strokes	n = 115
13a.		Positive first strokes (log scale)	n = 25
13b.		Positive first strokes (linear scale)	n = 25
14a.		Negative first strokes (log scale)	n = 90
14b.		Negative first strokes (linear scale)	n = 90
15.		Consecutive strokes	n = 88

Table VIII: (continued)

16.	Current peak over duration of flash	For all flashes	n = 118
17.		Positive strokes	n = 25
18.		Negative strokes	n = 93
19.	Current peak over front duration	First strokes	n = 106
20.		Positive first strokes	n = 18
21.		Negative first strokes	n = 88
22.	Current peak over time interval prior to stroke	Negative strokes	n = 132
23.	Total flash charge over flash duration	All flashes	n = 113
24.		Positive flashes	n = 25
25.		Negative flashes	n = 87
26.	Stroke charge over time interval prior to stroke	Negative strokes	n = 117
27.	Time interval over steepness of stroke	Negative strokes	n = 120

BIBLIOGRAPHY

1. K. BERGER and E. VOGELSANGER  
Measurements and results of research on lightning 1965-1963 on Mount San Salvatore  
Bull. ASE 56(1965)1, pp. 2-22
2. K. BERGER and E. VOGELSANGER  
Photographic investigation of lightning flashes in 1955-1965, on Mount San Salvatore  
Bull. ASE 57(1966)14, pp. 599-620
3. K. BERGER and E. VOGELSANGER  
New results of observation of lightning flashes  
Cigre report No. 33-03, 1968
4. S.A. PRENTICE  
Cigre lightning flash counters  
Electra (1972)22, pp. 149-171
5. K. BERGER  
The fundamental Principles of lightning protection  
Bull. ASE 61(1970)6, pp. 272 - 274

6. R.H. GOLDE  
Theoretical observations on the protection given by lightning conductors  
ETZ-A 82(1961)9, pp. 273-277
7. F. SCHWAB  
Calculation of the protective effect of lightning conductors and towers  
Bull. ASE 56(1965)17, pp. 678-683
8. H. BAATZ  
Radioactive isotopes do not improve protection against lightning  
ETZ-A 93(1972)2, pp. 101 - 104.  
Author's address: Prof. Dr. K. Berger, Gstadtstrasse 31, 8702 Zollikon, Switzerland

FIGURE CAPTIONS

- Fig. 1 Instruments on each of the two measuring towers T<sub>1</sub> and T<sub>2</sub>
- A Lightning aerial
  - FH Series gap
  - CA Triggering capacitor 0.25  $\mu$ F (Tower 1), 0.5  $\mu$ F (Tower 2).
  - S<sub>1</sub> Measuring shunt 0.8 ohm (Tower 1), 0.56 ohm (Tower 2), for long-duration lightning currents
  - S<sub>2</sub> Measuring shunt 0.05 ohm for impulse currents (Towers 1 and 2)
  - R<sub>1</sub> Measuring resistor, SO Loop 300 A range, 4.5 k ohm
  - R<sub>2</sub> Measuring resistor, SO Loop 5,000 A range, 7.0 k ohm
  - R<sub>3</sub> Measuring resistor, glow current measurement 0 - 10 mA, 1 k ohm
  - T Tower Structure
  - K<sub>1</sub> Old measuring cable, containing co-axial conductors, K 11 - K 13 for determining long duration currents, for triggering the oscillograph and providing primary illumination for the cathode ray oscillograph (KO).
  - K<sub>2</sub> Sheathed cable for triggering the rapid time base of KO
  - K<sub>3</sub> Sheathed cable for measuring the impulse current by means of the KOs
  - AL Aluminium protective tube in the ground as outermost screen
  - E Earth, consisting of the parallel earthing devices of the lightning measuring station, the Post Office equipment earth system, the cable car earth system and the water mains on San Salvatore.

In the rest position the lightning aerial is separated by the arcing horn (FH) from the measuring shunts. Small glow currents

Fig. 1 (continued)

are passed to a recording milliammeter by means of  $R_3$  and  $K_{11}$ . At an aerial current of about 7 A, the voltage drop at  $R_3$  becomes such that the threshold voltage (10 kV) of FH is reached and the aerial is connected to the measuring shunts. The voltage jump at  $R_3$  also triggers the loop oscillograph and the primary illumination of the cathode ray oscillograph. Short current impulses due to displacement currents, in the case of major field changes, are stored in the triggering capacitor (CA) without the oscillograph being triggered.

Fig. 2 The measuring equipment in the lightning current test room of "Antico Albergo"

- FK Faraday cage
- E Earthing of the entire installation on Mount San Salvatore
- $K_1-K_3$  Supply cables from tower 1, i.e.
  - $K_1$  Old measuring cable containing the co-axial conductors il-13 for current measurement by SO
  - $K_2$  Corrugated sheath co-axial cable for triggering the rapid time base of KO
  - $K_3$  Corrugated sheath co-axial cable for measuring impulse currents using the KO
- $K_4-K_6$  Connecting cables to the test room in the church and to the field mill in tower 1, i.e.
  - $K_4$  Remote control cable to the test room in the church
  - $K_5$  Corrugated sheath co-axial cable to field mill in tower 1
  - $K_6$  Post Office telephone cable to the test room in the church
- The following form part of the cathode ray oscillogram:
  - $P_1 P_2$  KO measuring plates for 65 kA and 200 kA ranges
  - $P_3$  Measuring plates for electrical field measurement (tower 1 only) 18 m above base of tower 1
- $VK_1, VK_2$  Delay cables
  - Z Terminating resistors of cables
  - M Electronic trigger for 1 s illumination (primary illumination) of KO
  - N Electronic trigger for time base and full illumination of KO
- The following are parts of the loop oscillograph SO
  - $SP_1, SP_2$  A storage circuit for measuring positive and negative impulse current maxima up to 200 kA, using the SO
  - $Sch_1, Sch_2$  Loops for measuring positive and negative impulse current maxima up to 200 kA using the SO
  - $Sch_3, Sch_4$  Loops of SO for measuring long-duration lightning currents of the current ranges 300 and 5000 A
  - L Triggering unit for SO loop illumination

- G Recording milliammeter for measuring small glow and displacement currents in the lightning aerial
- W Frequency modulator for transmitting measured glow and displacement currents of areas 7 mA and 1A to the magnetic memory of the field mill in the test room at the church
- V Line amplifier for frequency-modulated transmission

Fig. 3 Measuring tower No. 1

- a) Field mill, 1967, on the south eastern face of the tower; at the foot of the tower, the post office transmitter building
- b) Field mill 1967 on the side of the tower ("old field mill"), limit frequency 1200 Hz

Fig. 4 Diagram showing combined field mill with addition of two 180° measuring sectors, 180° aperture and 180° screening in the rotating disc

- Q<sub>1</sub> Electrostatic charge of sector 1
- Q<sub>2</sub> Electrostatic charge of sector 2
- T Cycle

Fig. 5 Diagram showing a combined field mill with addition of three 120° measuring sectors with 120° aperture and 240° screening in the rotating disc ("new field mill 1969")

- Q<sub>1</sub> Electrostatic charge of sector 1
- Q<sub>2</sub> Electrostatic charge of sector 2
- Q<sub>3</sub> Electrostatic charge of sector 3
- T Cycle

Fig. 6 Photograph of the new field mill, model 1969, in accordance with Figs. 5 and 7

- a) View from below showing the two 60° apertures
- b) Field mill, open

Fig. 7 Diagram of combined field mill ("new field mill") with remote control FE for driving, calibration, and zero line, with transducer W-V for transmission

- MP Field measurement plate segments
- B Screening plate (rotating disc)
- AM Asynchronous motor
- R Ring with 6 reed relays
- H Heating system
- GR Feed rectifier, stabilised
- E Summation amplifier, nexus type.

Fig. 7 (continued)

CL	Load capacitance of field mill
Cal	Calibration voltage source, stabilised with zener diodes
PR(1-3)	Parallel switching relay
ER	Earth relay
CR(1, 2)	Calibrating relay
T	Potentiometer with change-over switch
KR	Channel selector relay for two sensitivities
FE	Remote control receiver and transducer
K <sub>1</sub>	Feeder cable 200 V + 0 + E
K <sub>2</sub>	Post Office telephone cable for data transmission

Fig. 8 Circuit diagram of field measuring installations

MK	Test room at the church, San Salvatore
FM	Field mills, Salvatore 1 = new field mill, Salvatore 2 = old field mill
W	Modulator for converting the data into a frequency modulated signal which can be transmitted without interference via Post Office telephone cables
V	Line amplifier
MV	Amplifier of the old field mill Salvatore 2 on Tower 1
BSp 1-7	Magnetic tape memory, 7 places for 5 s
LV 1-7	Power amplifier for SO loops
Sch <sub>1</sub> -Sch <sub>4</sub>	Measuring loops for new field mills
Sch <sub>5</sub>	Measuring loop for old field mill
Sch <sub>6</sub> -Sch <sub>7</sub>	Measuring loops for glow currents up to 7 mA or 1A
ST	Timing device (measurement - calibration - zero line)
Osz	Loop oscillograph
K <sub>4</sub>	Remote control cable from the test room 'Antico Albergo'
K <sub>5</sub>	Coaxial cable to test room 'Antico Albergo'.
K <sub>5a</sub>	Corrugated sheath coaxial cables to field mill, Tower 1
K <sub>5b</sub>	Coaxial cable to potentiometer and tape store
K <sub>6</sub>	Post Office telephone cable for transmitting glow current data from the test room at 'Antico Albergo'.
K <sub>7</sub>	Post Office telephone cable from FM Agra to the centre at Lugano, 3.73 km, diameter 0.4/06 and 3.46 km, diameter 0.8
K <sub>8</sub>	Post Office telephone cable from FM Gemmo to the Lugano centre 1.49 km, diameter 0.6/0.8
K <sub>9</sub>	Post Office telephone cable from FM Pugerna to the Lugano centre, 4.53 km, diameter 0.6

Fig. 8 (continued)

K<sub>10</sub> Post Office telephone and sound cable from Lugano centre, to Monte San Salvatore, 4.13 km, diameter 1.0.

K<sub>11</sub> Coaxial cable of the new field mill on the church roof at San Salvatore to the tape store

Fig. 9 Number of thunderstorm days (isoceraunic level) from observations on Mount San Salvatore 1963-1971

Curves 1-9 Thunderstorm days of the years 1963-1971

Curve 10 Average for 9 years

n Thunderstorm days per month

t Calendar months

Fig.10 Variation of lightning current

a First stroke

b-g Second to nth stroke (Consecutive strokes)

Fig.11 Frequency of lightning currents of various intensity of all positive strokes

n Number of determinations

Fig.12 Frequency of lightning currents of various intensity of all negative strokes

n Number of measurements

Fig.13 Frequency of lightning currents of various intensity of all first strokes

n Number of determinations

Fig.14 Frequency of lightning currents of various intensity of all strokes

n Number of determinations

Fig.15 Frequency of various front durations T of all positive strokes

n Number of determinations

Fig.16 Frequency of various front durations T of all negative strokes

n Number of determinations

Fig.17 Frequency of various steepnesses  $di/dt$  of lightning current in positive strokes

n Number of determinations

Fig. 18 Frequency of various steepnesses  $di/dt$  of lightning current in negative strokes

$n$  = Number of determinations

Fig. 19 Frequency of various steepnesses  $di/dt$  of lightning current in all first strokes.

$n$  = Number of determinations.

Fig. 20 The frequency of various steepnesses of lightning current

$n$  = number of determinations.

Fig. 21 Correlation between the peak  $i$  and the steepness  $di/dt$  of positive first strokes

$n$  = number of determinations

Fig. 22 Correlation between the peak  $i$  and the steepness  $di/dt$  of negative first strokes

$n$  = number of determinations

Fig. 23 Correlation between the peak  $i$  and the steepness  $di/dt$  of all first strokes

$n$  = number of determinations

Fig. 24 Correlation between the peak  $i$  and the steepness  $di/dt$  of all consecutive strokes

$n$  = number of determinations

Fig. 25 Correlation between the peak  $i$  and the charge  $Q$  of the first positive strokes

$n$  = number of determinations

Fig. 26 Correlation between the peak  $i$  and the charge  $Q$  of negative first strokes

$n$  = number of determinations

Fig. 27 Correlation between the peak  $i$  and the charge  $Q$  of all first strokes

$n$  = number of determinations

Fig. 28 Correlation between the peak  $i$  and the charge  $Q$  for total flashes

$n$  = number of determinations

Fig. 29 Amplitude spectrum of lightning current in accordance with oscillograms No. 63072 and 70062

$n$  = number of determinations

Illustrations are reproduced by an economical method which is adequate for most purposes. If greater definition is required, please refer to the original document obtainable from the Library.

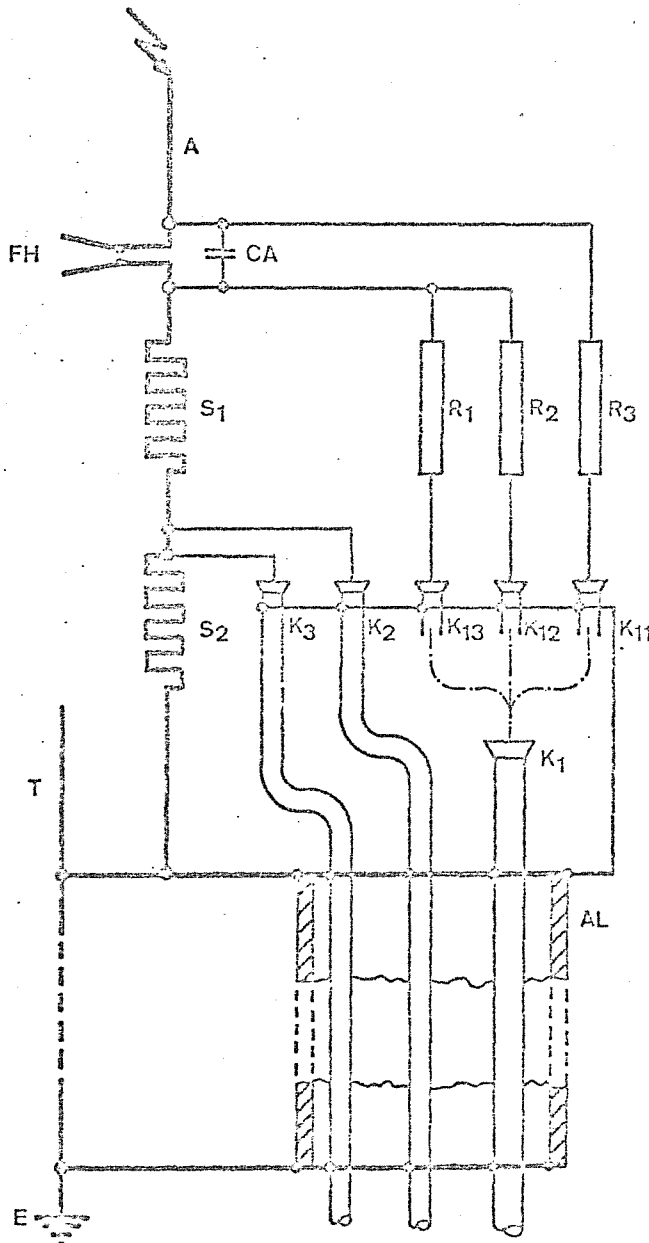


Fig. 1.

Fig. 1

Einrichtungen auf jedem der beiden Messtürme T<sub>1</sub> und T<sub>2</sub>

- A Blitzantenne
- FH Funkenstrecke
- CA Auslösekondensator 0,25 μF (Turm 1), 0,5 μF (Turm 2)
- S<sub>1</sub> Mess-Shunt 0,8 Ω (Turm 1); 0,56 Ω (Turm 2), für langdauernde Blitzströme
- S<sub>2</sub> Mess-Shunt 0,05 Ω für Stoßströme (Turm 1 und Turm 2)
- R<sub>1</sub> Messwiderstand zu SO-Schleife 300-A-Bereich, 4,5 kΩ
- R<sub>2</sub> Messwiderstand zu SO-Schleife 5000-A-Bereich, 7,0 kΩ
- R<sub>3</sub> Messwiderstand für Glühstrommessung 0...10 mA, 1 kΩ
- T Turmstruktur
- K<sub>1</sub> altes Messkabel, enthaltend die Koaxialadern K 11...K 13 zur Messung der langdauernden Ströme, zur Auslösung des Schleifenoszillographen und zur Grundaufteilung des Kathodenstrahlloszillographen (KO)
- K<sub>2</sub> Wellmantelkabel zur Auslösung der raschen Zeitablenkung des Kathodenstrahlloszillographen
- K<sub>3</sub> Wellmantelkabel zur Messung der Stoßströme mit den Kathodenstrahlloszillographen
- AL Aluminiumschutzrohr, bzw. Zoreskanal im Erdboden als äusserster Schirm
- E Erdung, bestehend aus den parallelgeschalteten Erdungsnetzen der Blitzmessstation, der PTT-Anlageerde, dem Erdungsnetz der Seilbahnanlage und dem Wasserleitungsnetz auf dem San Salvatore

Im Ruhezustand ist die Blitzantenne durch das Funkenhorn (FH) von den Mess-Shunts getrennt. Kleine Glühströme werden über R<sub>3</sub> und K<sub>11</sub> einem Registrier-Milliampèremeter zugeführt. Bei einem Antennenstrom von ca. 7 A wird der Spannungsabfall an R<sub>3</sub> so hoch, dass die Ansprechspannung (10 kV) des Funkenhorns (FH) erreicht wird; dadurch wird die Antenne an die Mess-Shunts geschaltet. Der Spannungssprung an R<sub>3</sub> dient gleichzeitig auch der Auslösung des Schleifenoszillographen und der Grundaufteilung des Kathodenstrahlloszillographen. Kurze Stromimpulse, entstanden durch Verschiebungsströme bei grossen Feldänderungen, werden im Auslösekondensator (CA) gespeichert, ohne dass eine Auslösung des Oszillographen erfolgt. Das Schema bezieht sich sinngemäss auf die Einrichtung pro Messturm.

Fig. 2.

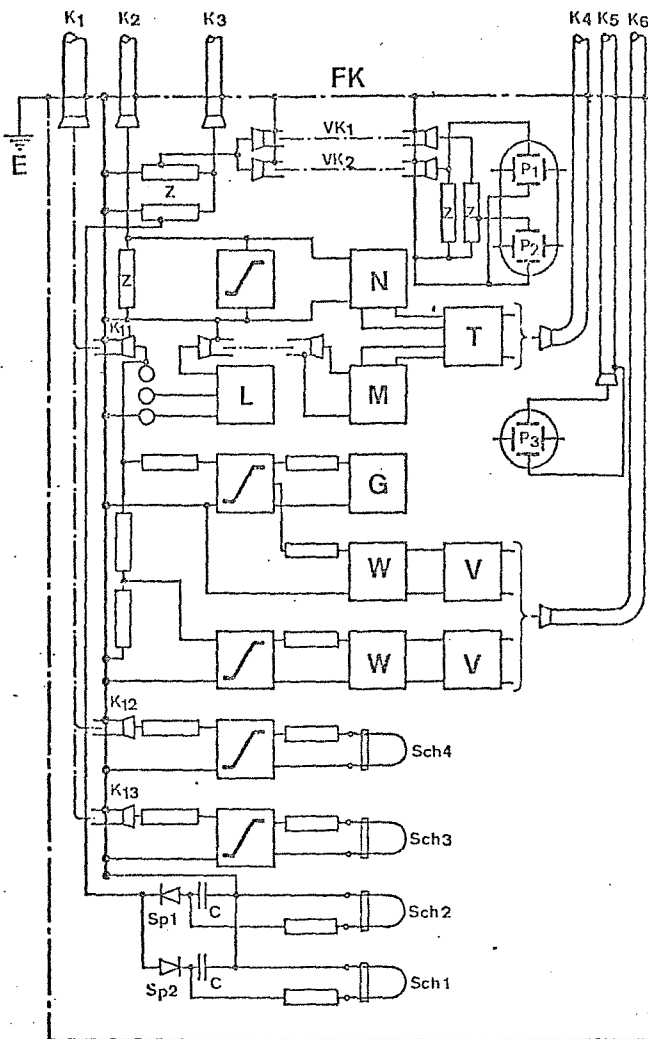


Fig. 2

Messeinrichtungen im Blitzstrom-Messraum des «Antico Albergo»

- FK Faraday-Käfig
- E Erdung der gesamten Anlagen auf dem San Salvatore
- K<sub>1...K<sub>3</sub></sub> Zuleitungskabel vom Turm 1, nämlich:
  - K<sub>1</sub> Altes Messkabel, enthaltend die Koaxial-Adern 11...13 für Strommessung durch den SO
  - K<sub>2</sub> Wellmantel-Koaxialkabel zur Auslösung der raschen Zeitablenkung des KO
  - K<sub>3</sub> Wellmantel-Koaxialkabel zur Messung von Stoßströmen mit dem KO
- K<sub>4...K<sub>6</sub></sub> Verbindungskabel zum Messraum «Kirche» und zur Feldmühle Turm 1, nämlich:
  - K<sub>4</sub> Fernsteuerkabel zum Messraum «Kirche»
  - K<sub>5</sub> Wellmantel-Koaxialkabel zur Feldmühle Turm 1
  - K<sub>6</sub> PTT-Telephonkabel zum Messraum «Kirche»
- Zum Kathodenstrahloszillographen gehörend:
  - P<sub>1</sub>P<sub>2</sub> KO Messplatten für Bereiche 65 kA und 200 kA
  - P<sub>3</sub> Messplatten für elektrische Feldmessung (nur an Turm 1), 18 m über Turmbasis 1
  - VK<sub>1</sub>, VK<sub>2</sub> Verzögerungskabel
  - Z Abschlusswiderstände der Kabel
  - M Auslöseelektronik für 1-s-Aufhellung (Grundaufhellung) des KO
  - N Auslöseelektronik für Zeitablenkung und Vollaufhellung des KO
- Zum Schleifenoszillographen SO gehörend:
  - SP<sub>1</sub>, SP<sub>2</sub> Speicherschaltung zur Messung der positiven und negativen Stoßstrom-Maximalwerte bis 200 kA mit dem SO
  - Sch<sub>1</sub>, Sch<sub>2</sub> Meßschleifen zur Messung der positiven und negativen Stoßstrom-Maximalwerte bis 200 kA mit dem SO
  - Sch<sub>3</sub>, Sch<sub>4</sub> Meßschleifen des SO zur Messung langdauernder Blitzströme der Strombereiche 300 bzw. 5000 A
  - L Auslöse-Einheit für SO-Schleifenbeleuchtung
  - G Registrier-Milliamperemeter zur Messung kleiner Glimm- und Verschiebungsströme in der Blitzantenne
  - W Frequenzmodulator zur Übertragung gemessener Glimm- und Verschiebungsströme der Bereiche 7 mA bzw. 1 A auf den Magnetspeicher der Feldmühlemessungen im Messraum «Kirche»
  - V Linienverstärker für die frequenzmodulierte Übertragung

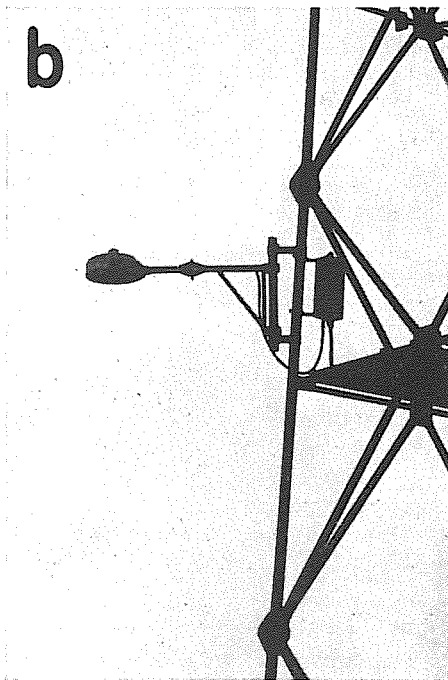
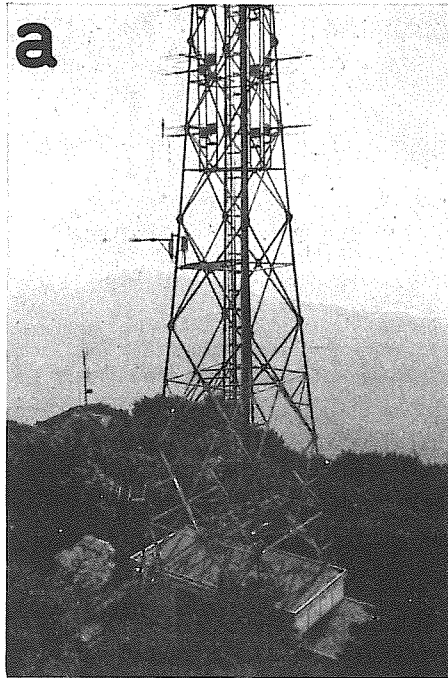


Fig. 3

Messturm 1

- a* Feldmühle 1967 an der SE-Turmflanke, am Turmfuss das Sendegebäude der PTT
- b* Feldmühle 1967 an der Turmflanke («alte Feldmühle»), Grenzfrequenz 1200 Hz

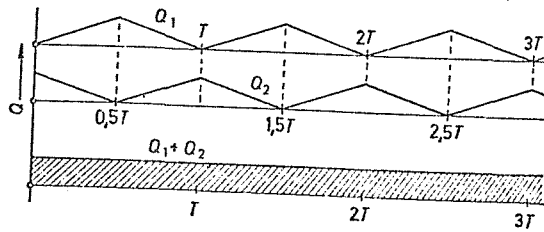


Fig. 4  
 Schematische Darstellung einer kombinierten Feldmühle  
 mit Addition zweier 180°-Meßsektoren, 180°-Öffnung und 180°-Ab-  
 deckung in der rotierenden Scheibe  
 $Q_1$  Influenzladung des 1. Sektors  
 $Q_2$  Influenzladung des 2. Sektors  
 $T$  Periodendauer

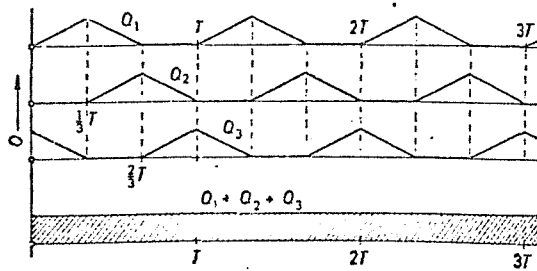


Fig. 5  
 Schematische Darstellung einer kombinierten Feldmühle  
 mit Addition dreier 120°-Meßsektoren mit 120°-Öffnung und 240°-Ab-  
 deckung in der rotierenden Scheibe  
 (=neue Feldmühle 1969.)  
 $Q_1$  Influenzladung des 1. Sektors  
 $Q_2$  Influenzladung des 2. Sektors  
 $Q_3$  Influenzladung des 3. Sektors  
 $T$  Periodendauer

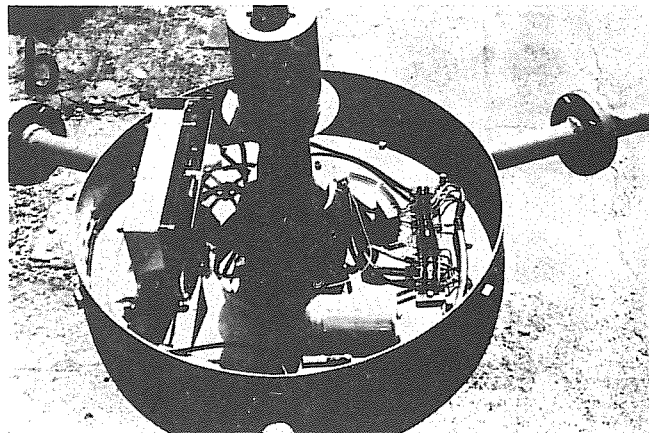
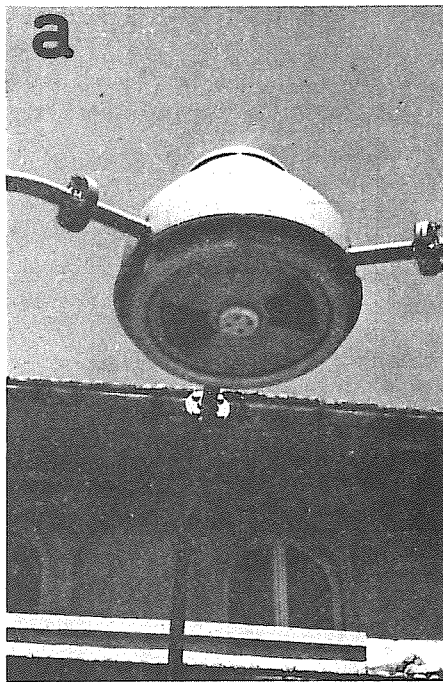


Fig. 6

Bild der neuen Feldmühle, Typ 1969, entsprechend den Fig. 5 und 7

- a Ansicht von unten auf die zwei 60°-Sektoröffnungen
- b Feldmühle geöffnet

Fig. 7.

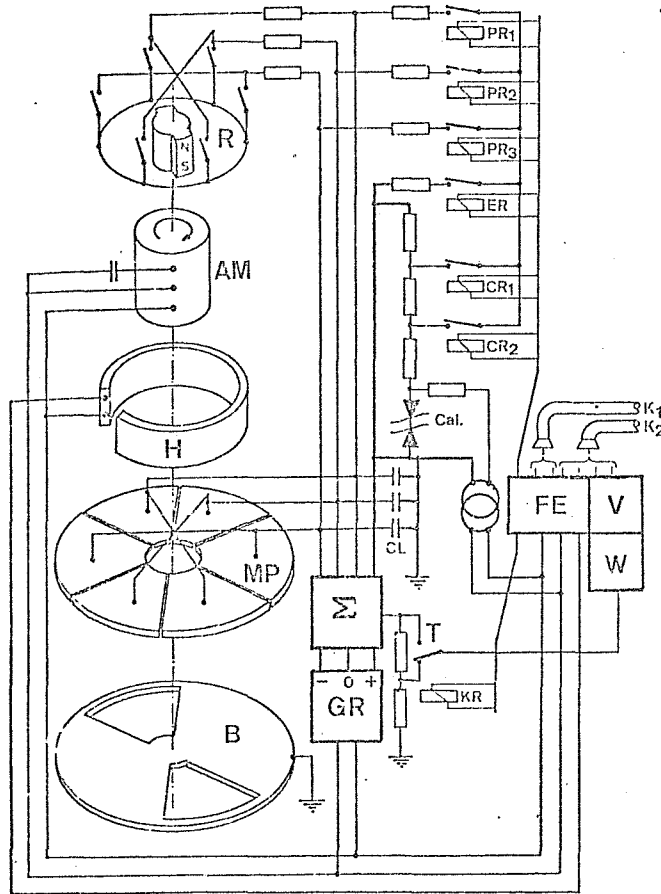


Fig. 7

Schema der kombinierten Feldmühle (neue Feldmühle) samt Fernsteuerung FE für Antrieb, Eichung und Nulllinie, mit Messumformer W-V zur Übertragung

- MP Feldmess-Plattensegmente
- B Abschirmplatte (rotierende Blende)
- AM Asynchronmotor
- R Ring mit 6 Read-Relais
- H Heizung
- GR Speisegleichrichter, stabilisiert
- Σ Summationsverstärker, Nexus-Typ
- CL Belastungskapazität der Feldmühle
- Cal Eichspannungsquelle, stabilisiert mit Zener-Dioden
- PR(1...3) Parallelschaltrelais
- ER Erdungsrelais
- CR(1,2) Eichrelais
- T Spannungsteiler mit Umschalter
- KR Kanal-Wahl-Relais für zwei Empfindlichkeiten
- FE Fernsteuerempfänger und Messwert-Umformer
- K<sub>1</sub> Speisekabel 200 V + 0 + E
- K<sub>2</sub> PTT-Telephonkabel für Messwert-Übertragung

Fig. 8.

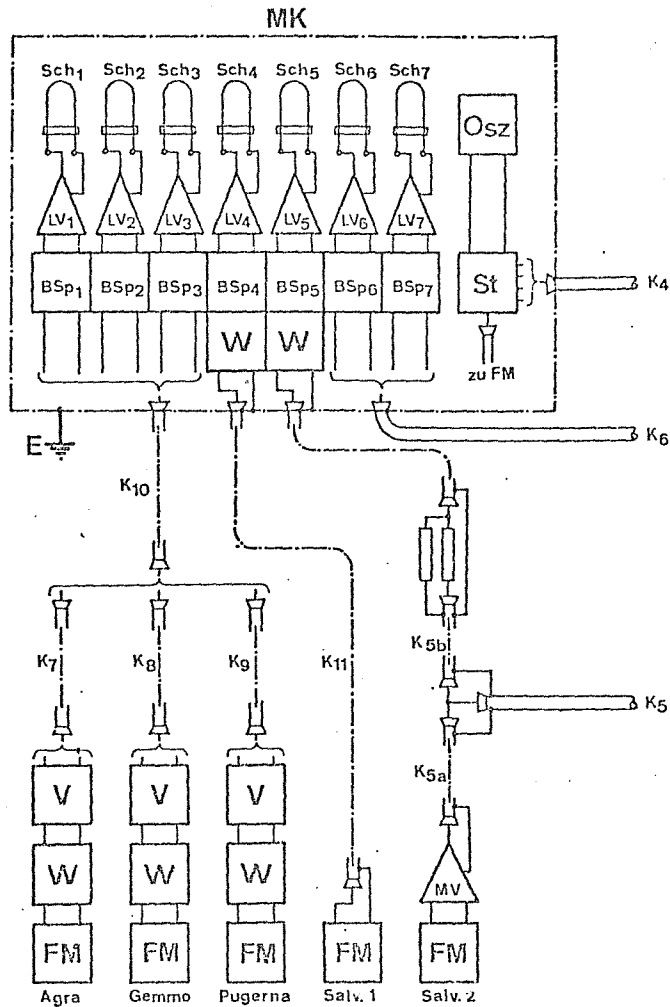


Fig. 8

Blockschema der Feldmess-Einrichtungen

- MK** Messraum «Kirche» San Salvatore
- FM** Feldmühlen, Salvatore 1 = neue Feldmühle, Salvatore 2 = alte Feldmühle
- W** Modulator zur Umwandlung der Messgrößen in ein frequenzmoduliertes Signal, welches störungsfrei über PTT-Telephonkabel übertragen werden kann
- V** Linienverstärker
- MV** Messverstärker der alten Feldmühle Salvatore 2 auf Turm 1
- BSp 1...7** Magnetbandspeicher, 7 Spuren für 5 s
- LV 1...7** Leistungsverstärker für SO-Schleifen
- Sch<sub>1</sub>...Sch<sub>4</sub>** Meßschleifen für neue Feldmühlen
- Sch<sub>5</sub>** Meßschleife für alte Feldmühle
- Sch<sub>6</sub>...Sch<sub>7</sub>** Meßschleifen für Glimmströme bis 7 mA bzw. 1 A
- St** Zeitsteuergerät für Funktionsablauf (Messung — Eichung — Nulllinie)
- OsZ** Schleifenzillograph
- K<sub>1</sub>** Fersteuerkabel vom Messraum «Antico Albergo»
- K<sub>5</sub>** Koaxialkabel zum Messraum «Antico Albergo»
- K<sub>5a</sub>** Wellmantel Koaxialkabel zur Feldmühle, Turm 1
- K<sub>5b</sub>** Koaxialkabel zum Spannungsteiler und Bandspeicher
- K<sub>6</sub>** PTT-Telephonkabel zur Übertragung der Glimmstrom-Messwerte aus dem Messraum «Antico Albergo»
- K<sub>7</sub>** PTT-Telephonkabel ab FM Agra bis Zentrale Lugano, 3,73 km,  $\phi$  0,4/0,6 und 3,46 km,  $\phi$  0,8
- K<sub>8</sub>** PTT-Telephonkabel ab FM Gemmo bis Zentrale Lugano 1,49 km,  $\phi$  0,6/0,8
- K<sub>9</sub>** PTT-Telephonkabel ab FM Pugerna bis Zentrale Lugano, 4,53 km,  $\phi$  0,6
- K<sub>10</sub>** PTT-Telephon- und Musikkabel ab Zentrale Lugano bis Monte San Salvatore, 4,13 km,  $\phi$  1,0
- K<sub>11</sub>** Koaxialkabel der neuen Feldmühle auf dem Kirchendach San Salvatore zum Bandspeicher

Fig. 9

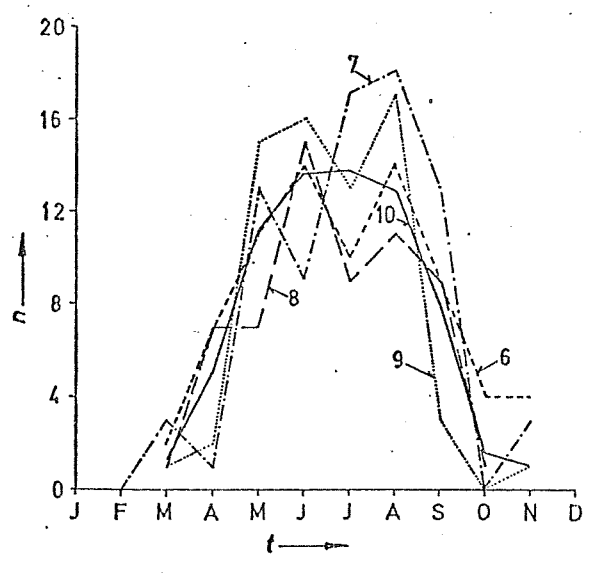
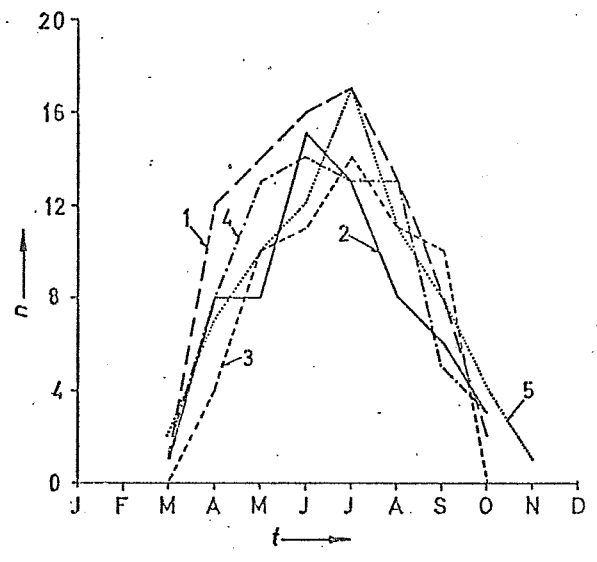
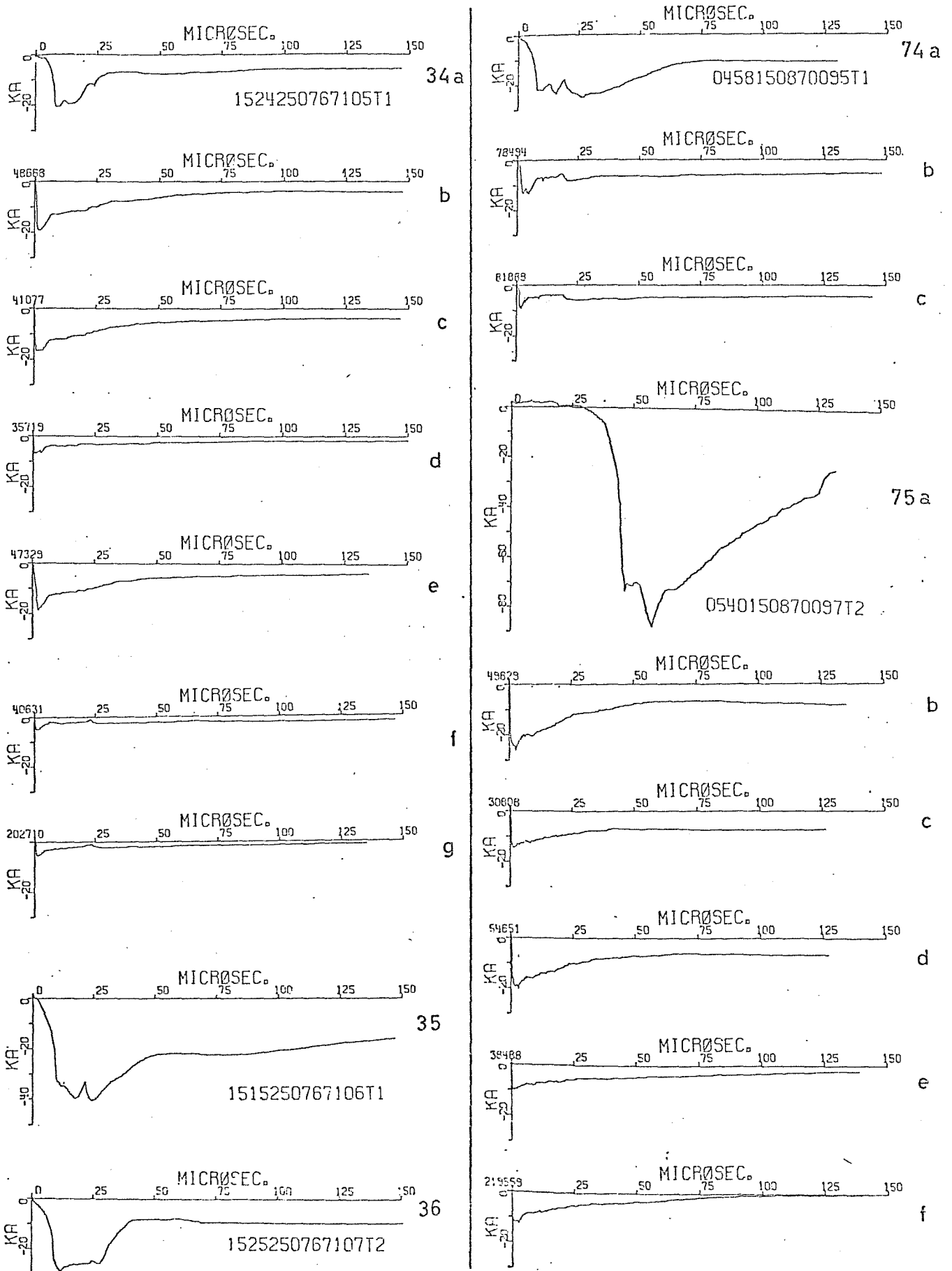


Fig. 9  
 Anzahl Gewittertage (isoceraunic level) nach den Beobachtungen  
 auf dem Monte San Salvatore 1963...1971  
 Kurve 1...9 Gewittertage jeden Jahres 1963...1971  
 Kurve 10 Mittelwert aller 9 Jahre  
 n Anzahl Gewittertage pro Monat  
 t Bezeichnung der Kalendermonate

Fig. 10  
Blitzstromverlauf

a erster Teilblitz  
b...g zweiter bis n-ter Teilblitz (Folgeblitze)



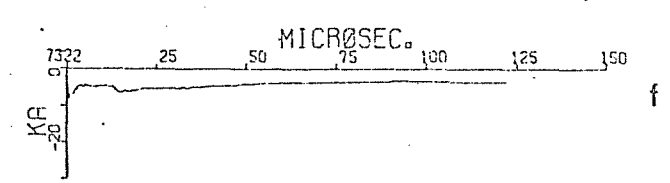
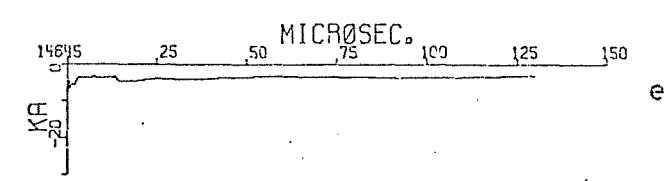
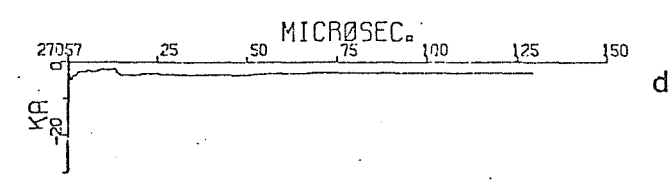
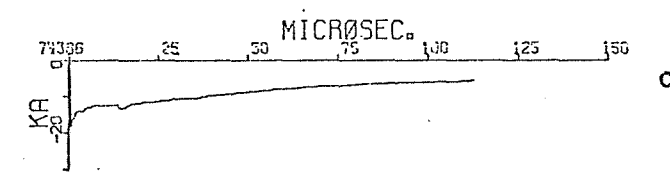
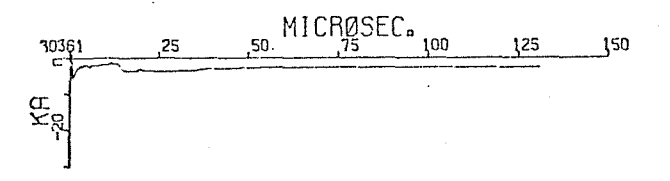
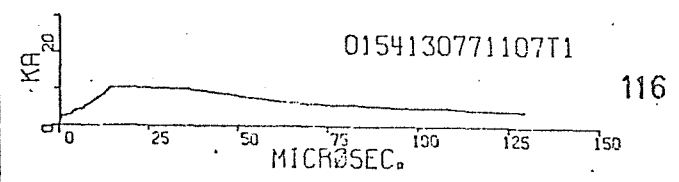
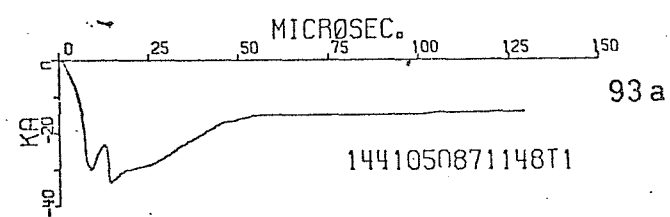
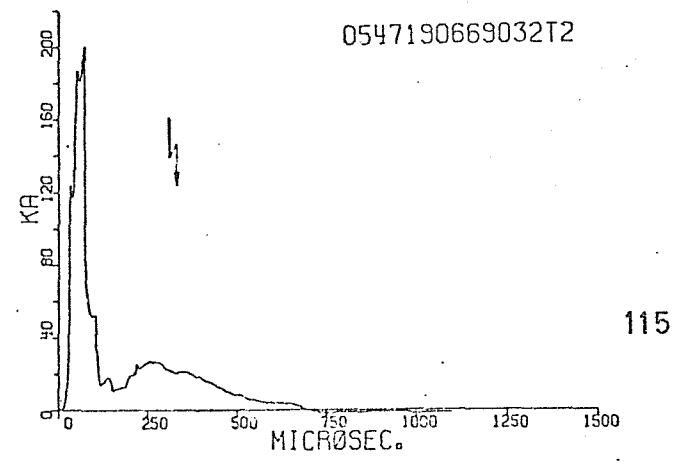
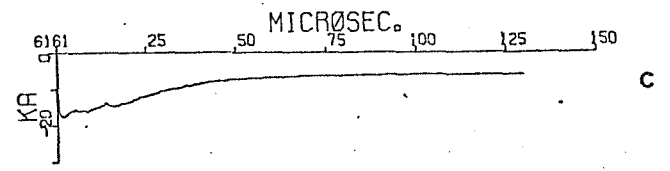
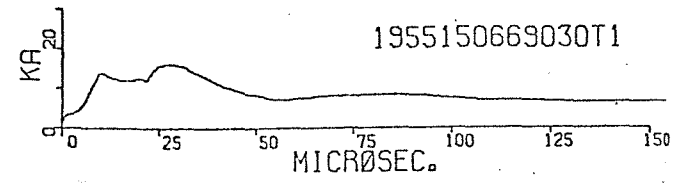
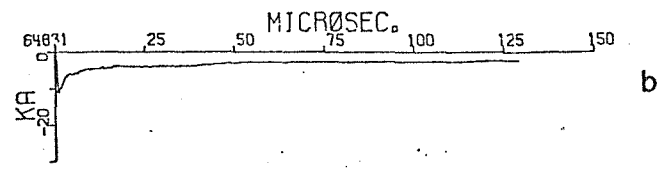
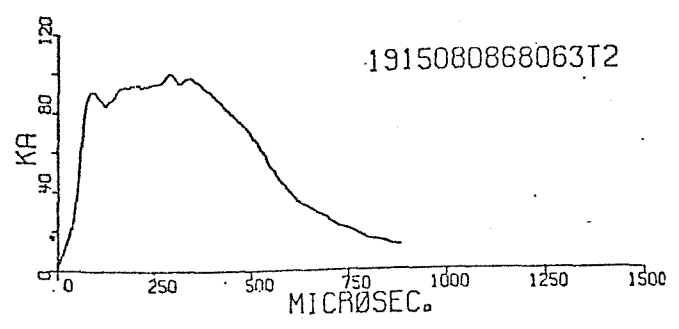
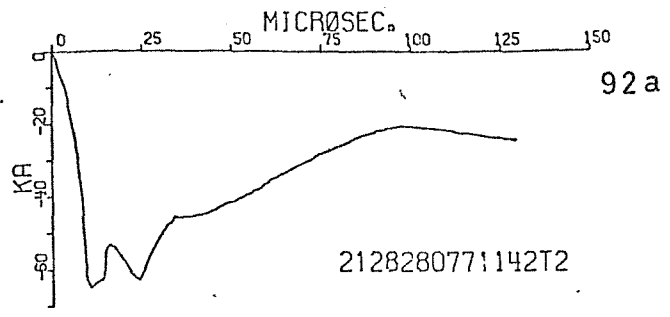


Fig. 10 (continued.)

Fig. 11.

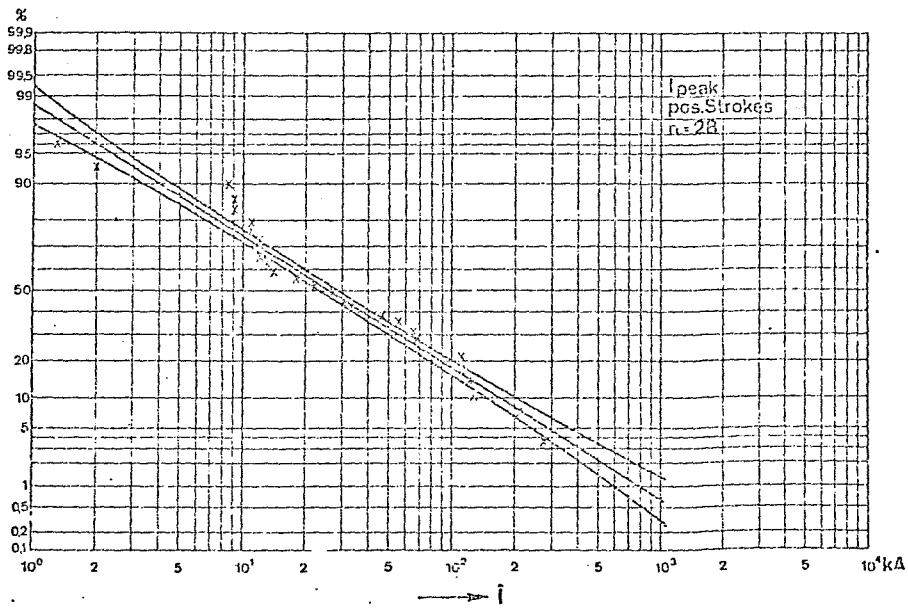


Fig. 11  
Häufigkeit verschieden hoher Blitzströme  $I_{peak}$   
aller positiven Teilblitze  
 $n$  Anzahl Messungen

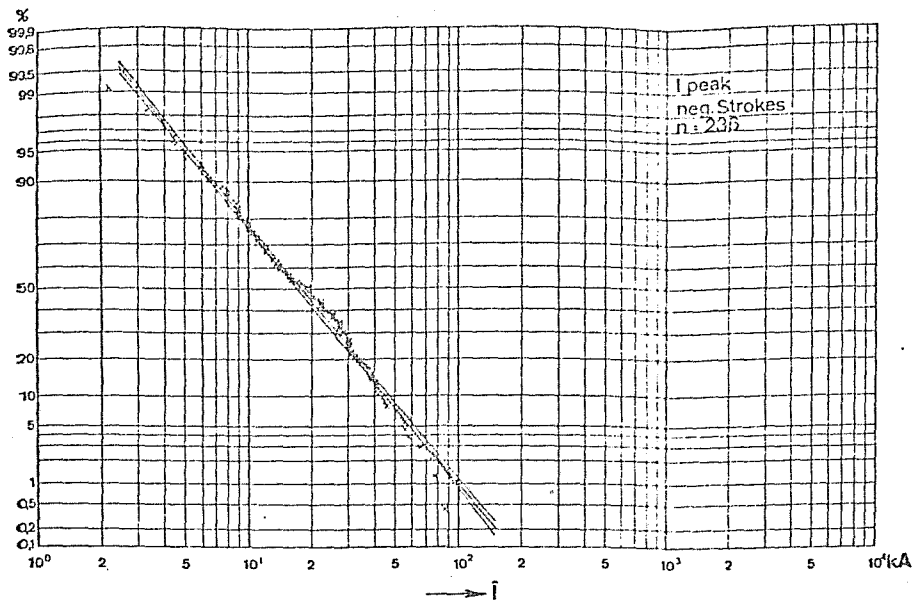


Fig. 12  
Häufigkeit verschieden hoher Blitzströme  $i$   
aller negativen Teilblitze  
 $n$  Anzahl Messungen

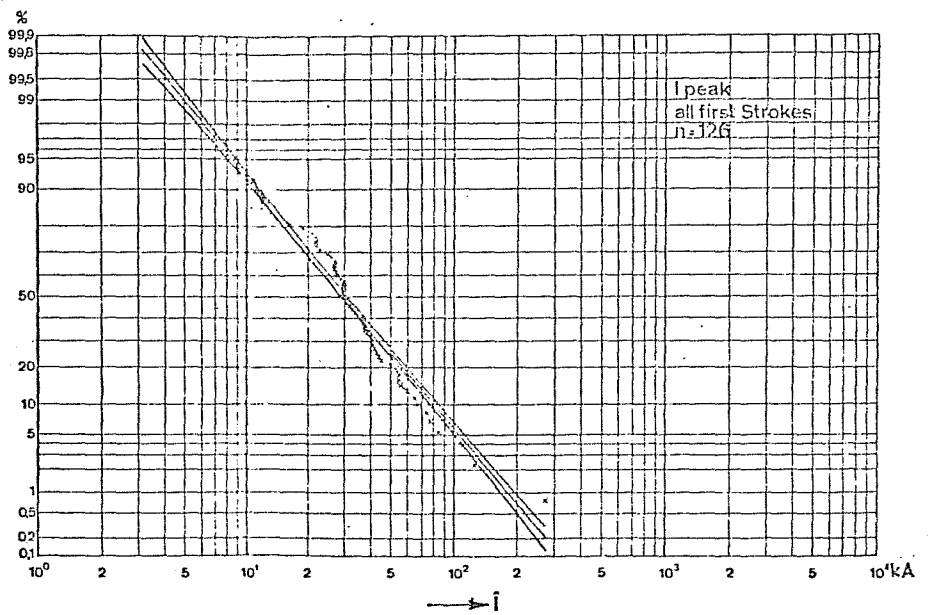


Fig. 13  
Häufigkeit verschieden hoher Blitzströme  $i$   
aller ersten Teilblitze  
 $n$  Anzahl Messungen

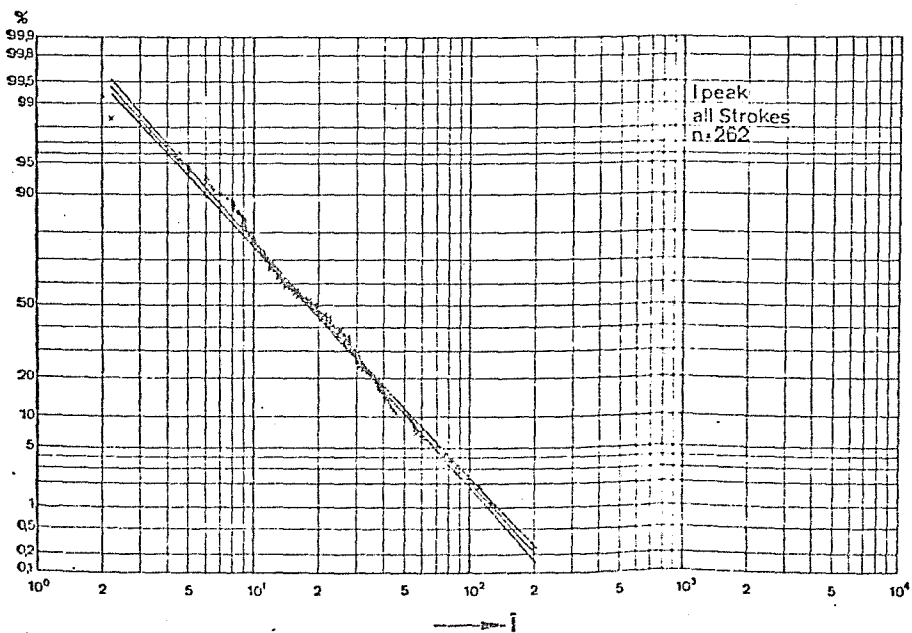


Fig. 14  
Häufigkeit verschieden hoher Blitzströme  $i$   
aller Teilblitze  
 $n$  Anzahl Messungen

Fig. 15.  
Häufigkeit verschiedener Frontdauern  $T$   
aller positiven Teilblitze  
 $n$  Anzahl Messungen

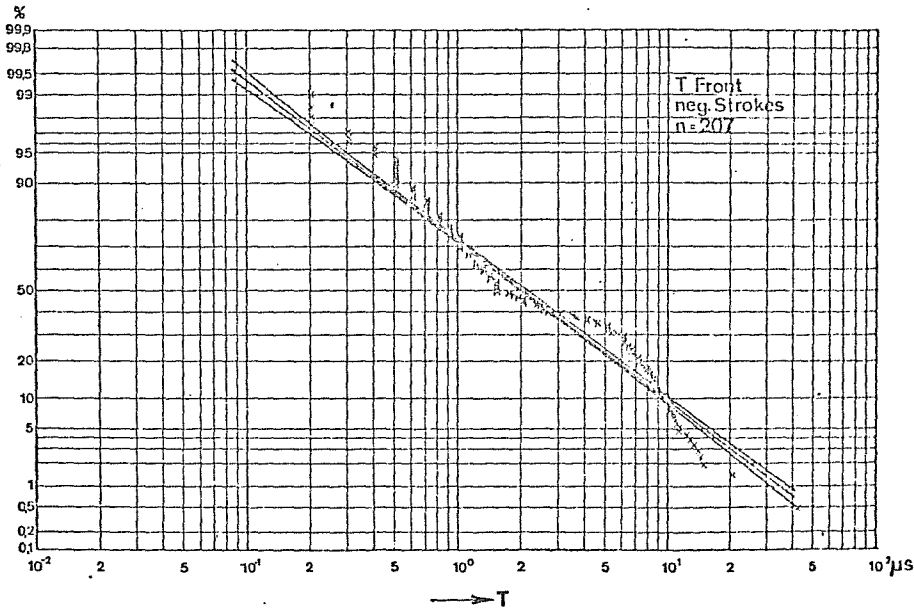
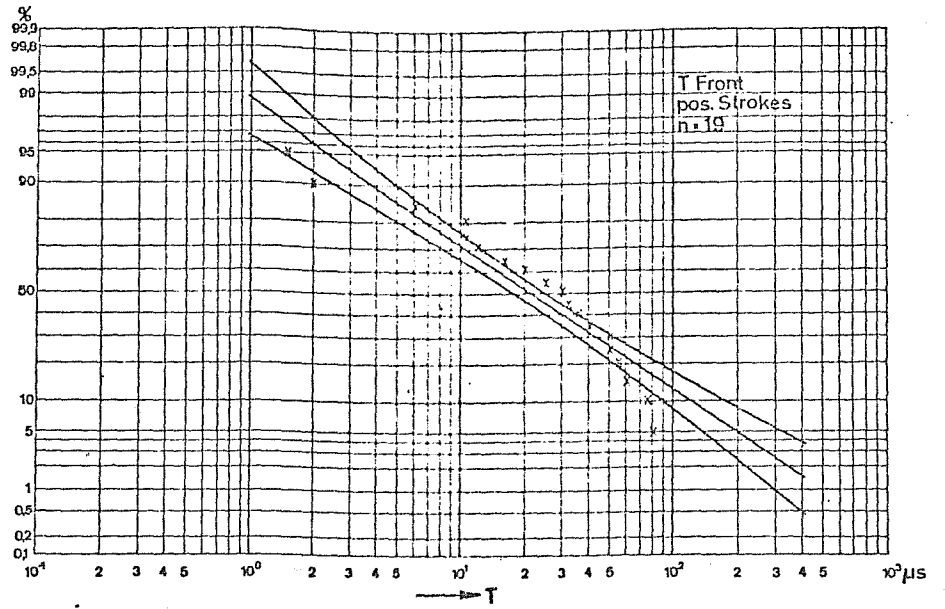


Fig. 16  
Häufigkeit verschiedener Frontdauern  $T$   
aller negativen Teilblitze  
 $n$  Anzahl Messungen

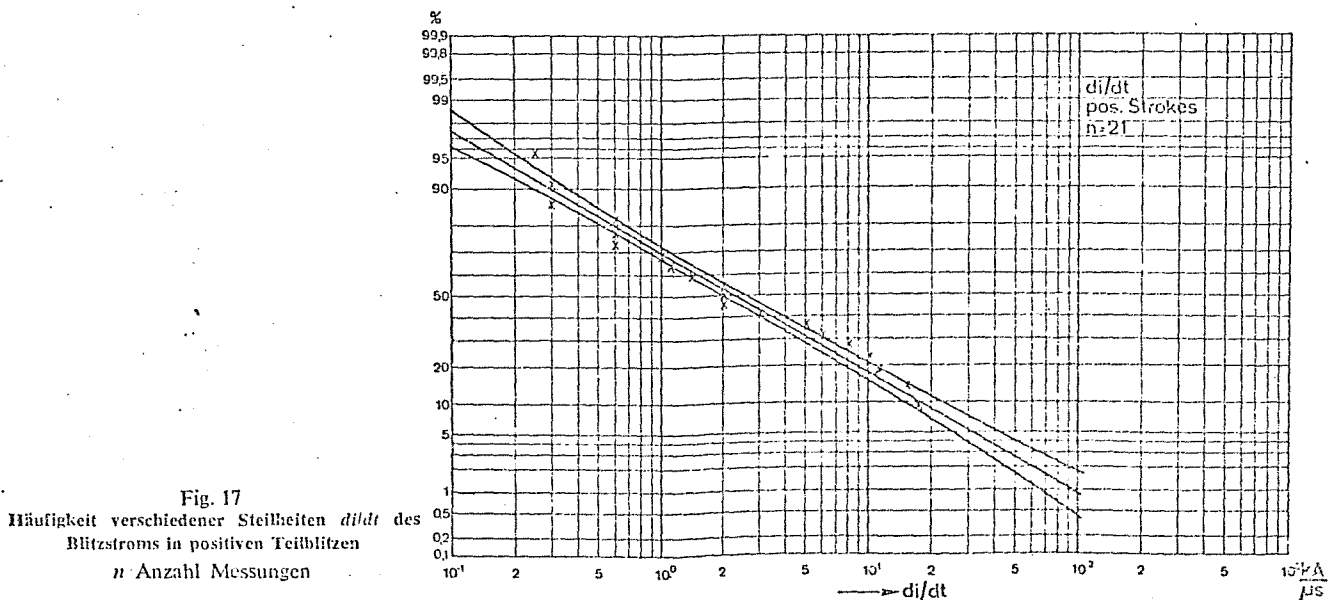


Fig. 17  
Häufigkeit verschiedener Steilheiten  $di/dt$  des  
Blitzstroms in positiven Teilblitzen  
 $n$  Anzahl Messungen

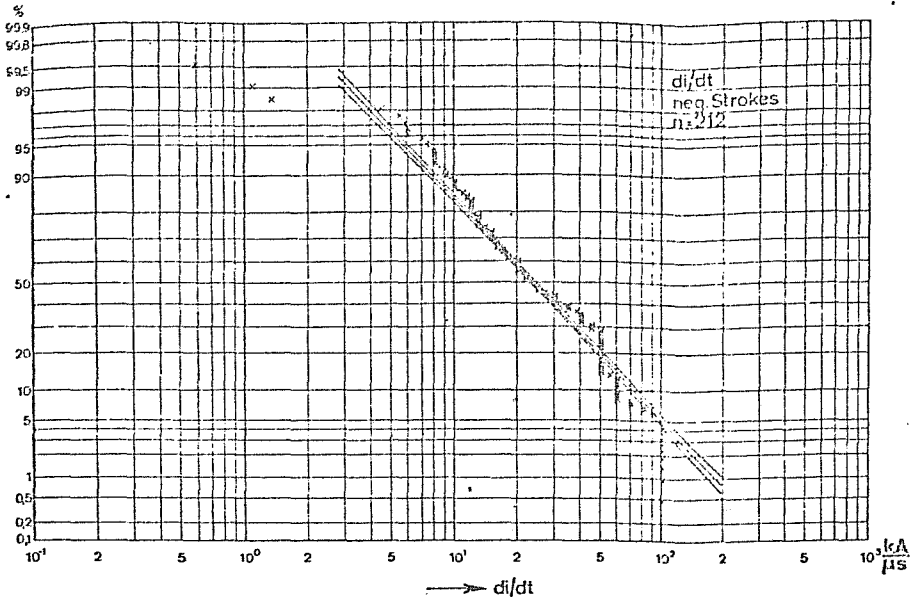


Fig. 18  
Häufigkeit verschiedener Steilheiten  $di/dt$  des  
Blitzstromes in negativen Teilblitzen  
 $n$  Anzahl Messungen

→  $di/dt$

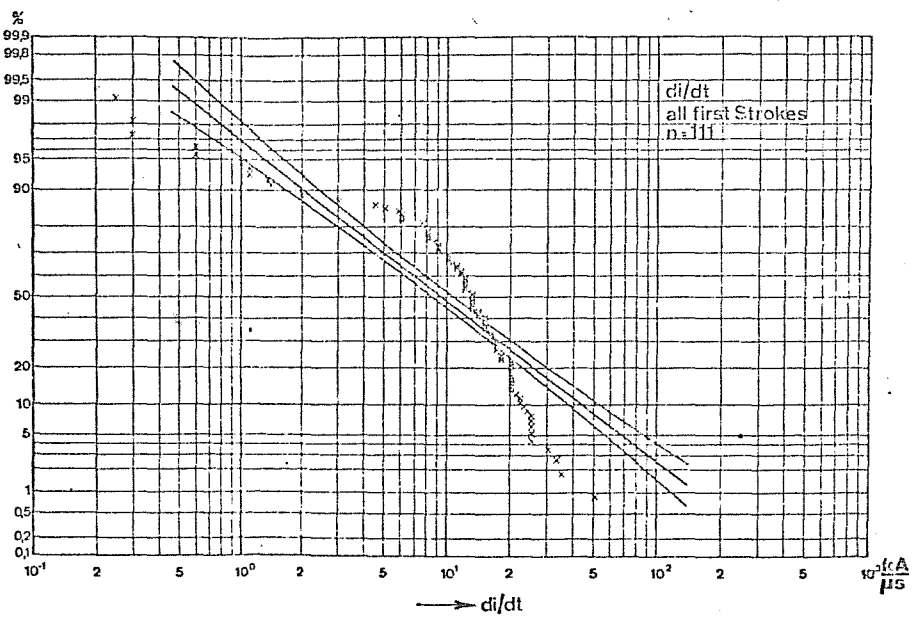


Fig. 19  
Häufigkeit verschiedener Steilheiten  $di/dt$  des  
Blitzstromes in allen ersten Teilblitzen  
 $n$  Anzahl Messungen

→  $di/dt$

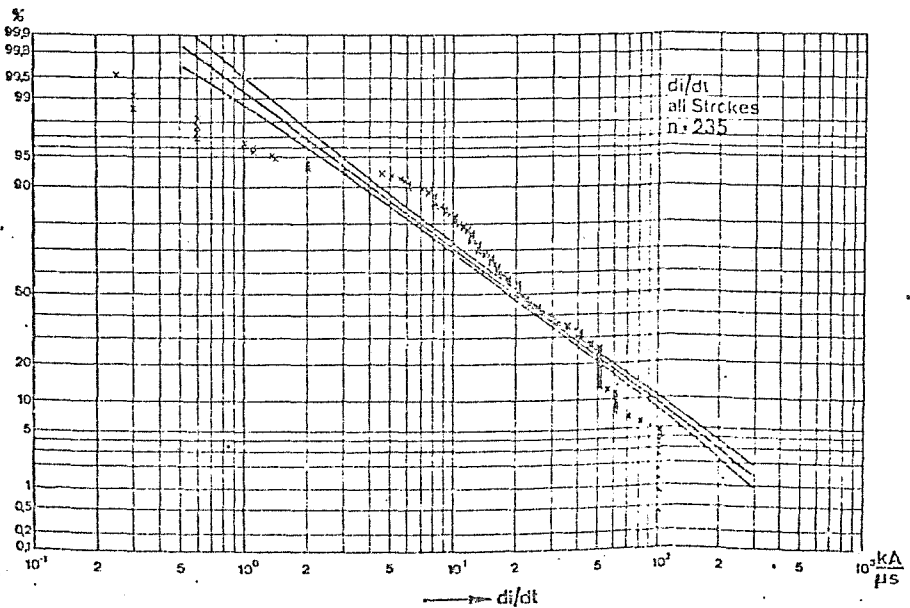


Fig. 20  
Häufigkeit verschiedener Steilheiten des  
Blitzstromes  
 $n$  Anzahl Messungen

→  $di/dt$

Fig. 21  
Korrelation zwischen Scheitelwert  $i$  und Steilheit  $di/dt$  von positiven ersten Teilblitzen  
 $n$  Anzahl Messungen

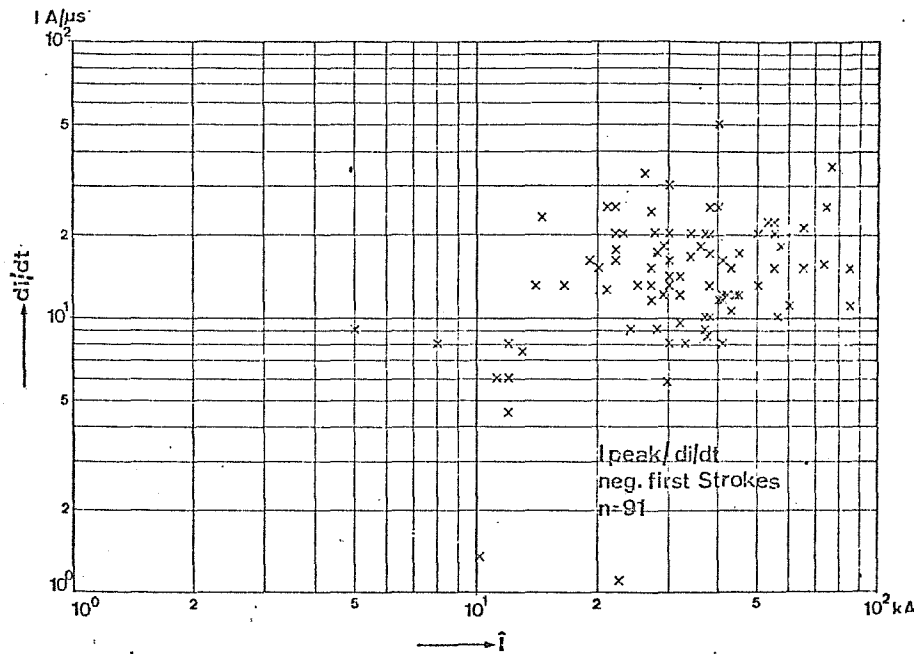
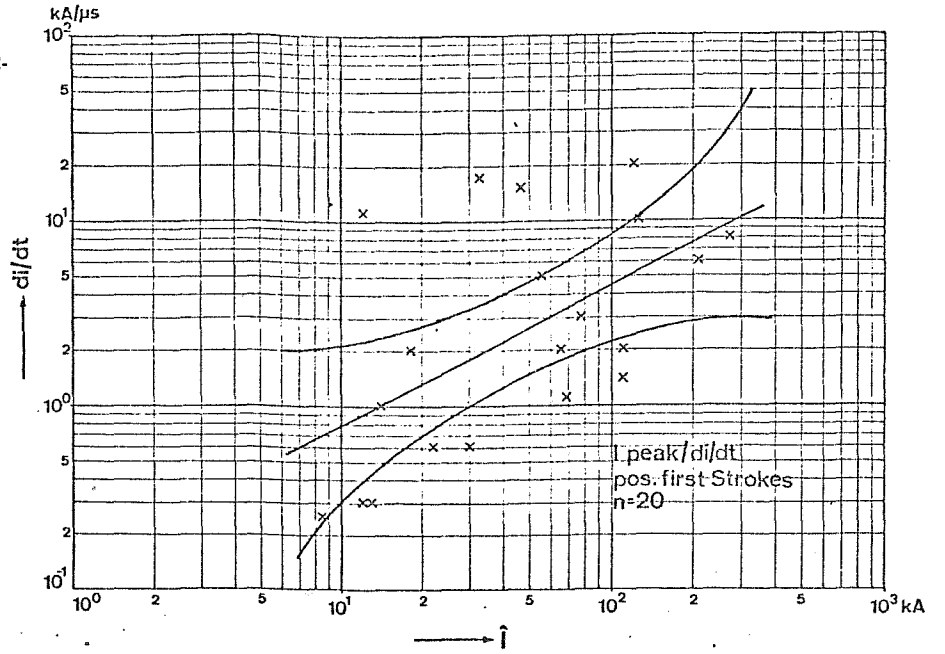
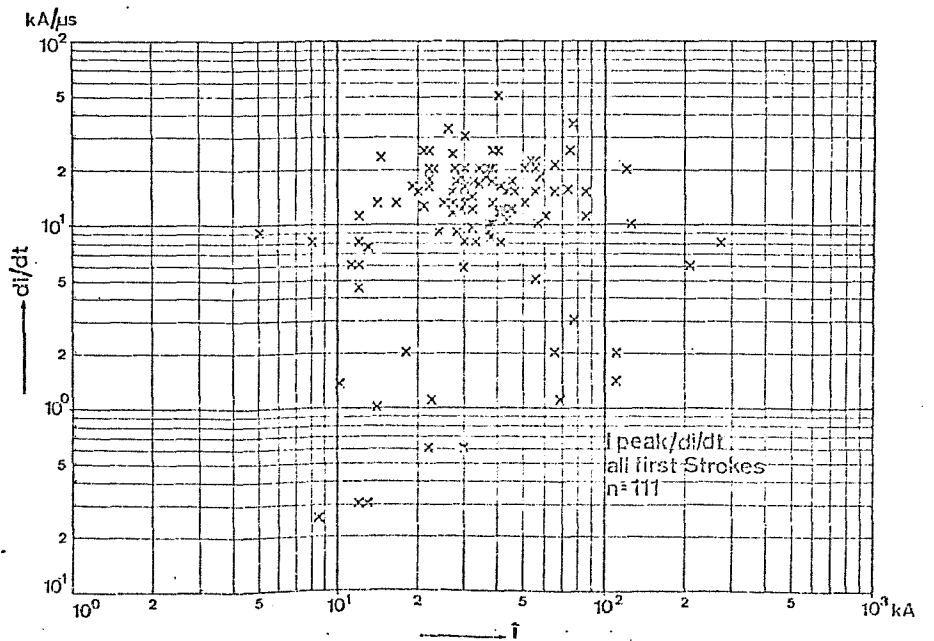


Fig. 22  
Korrelation zwischen Scheitelwert  $i$  und Steilheit  $di/dt$  von negativen ersten Teilblitzen  
 $n$  Anzahl Messungen

Fig. 23  
Korrelation zwischen Scheitelwert  $i$  und Steilheit  $di/dt$  von allen ersten Teilblitzen  
 $n$  Anzahl Messungen



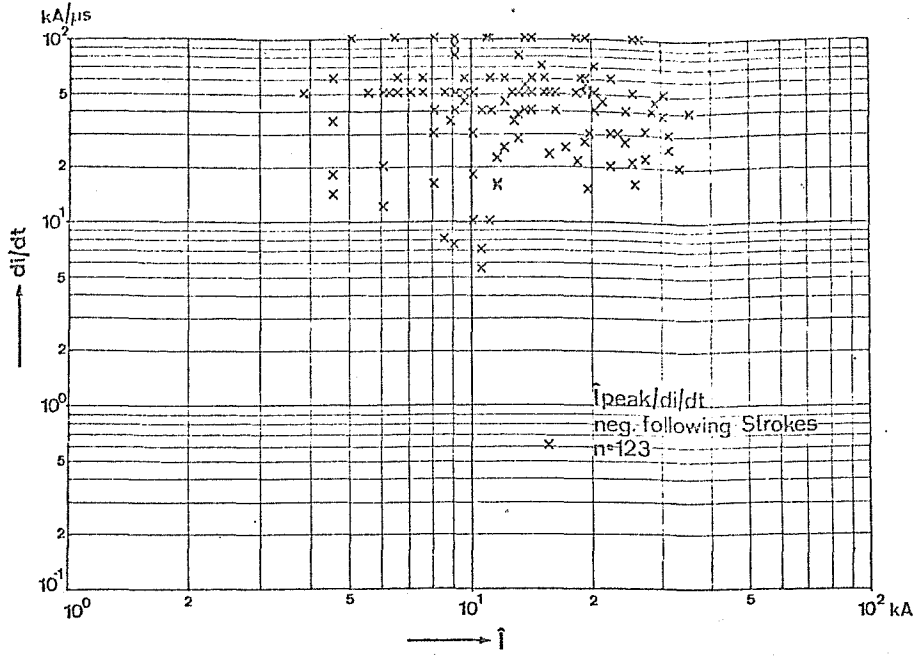


Fig. 24  
Korrelation zwischen Scheitelwert  $i$  und Steilheit  $di/dt$  von allen Folgeblitzen  
 $n$  Anzahl Messungen

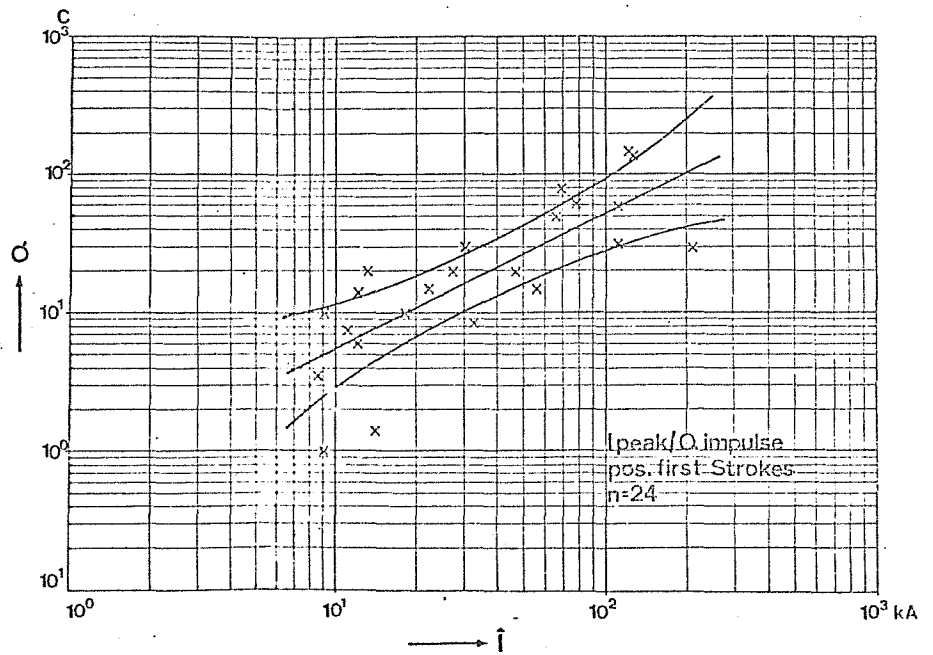


Fig. 25  
Korrelation zwischen Scheitelwert  $i$  und Ladung  $Q$  der ersten positiven Teilblitze  
 $n$  Anzahl Messungen

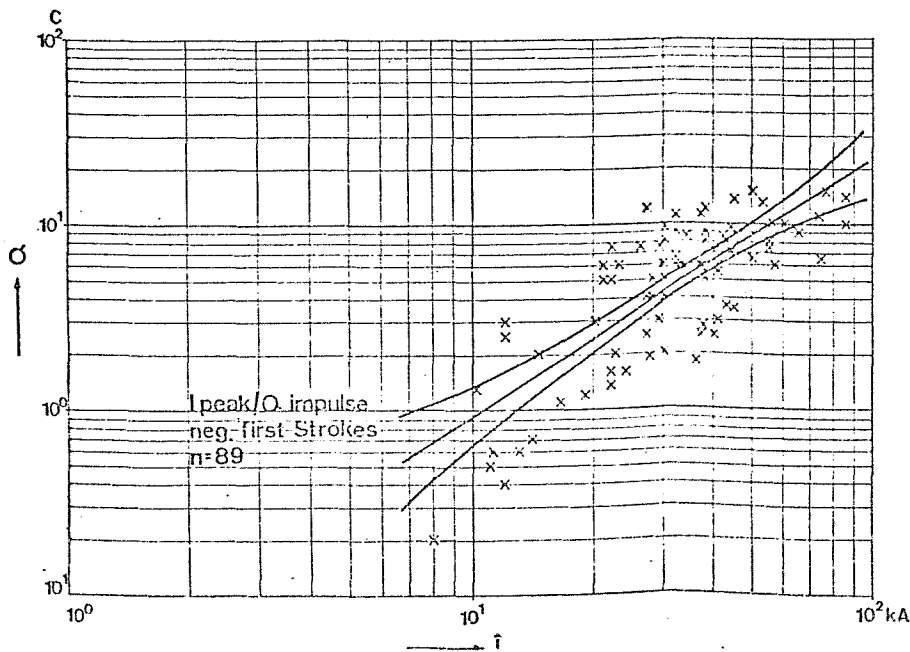


Fig. 26  
Korrelation zwischen Scheitelwert  $i$  und Ladung  $Q$  für den ersten negativen Teilblitz  
 $n$  Anzahl Messungen

Fig. 27  
Korrelation zwischen Scheitelwert  $i$  und  
Ladung  $Q$  für alle ersten Teilblitze  
 $n$  Anzahl Messungen

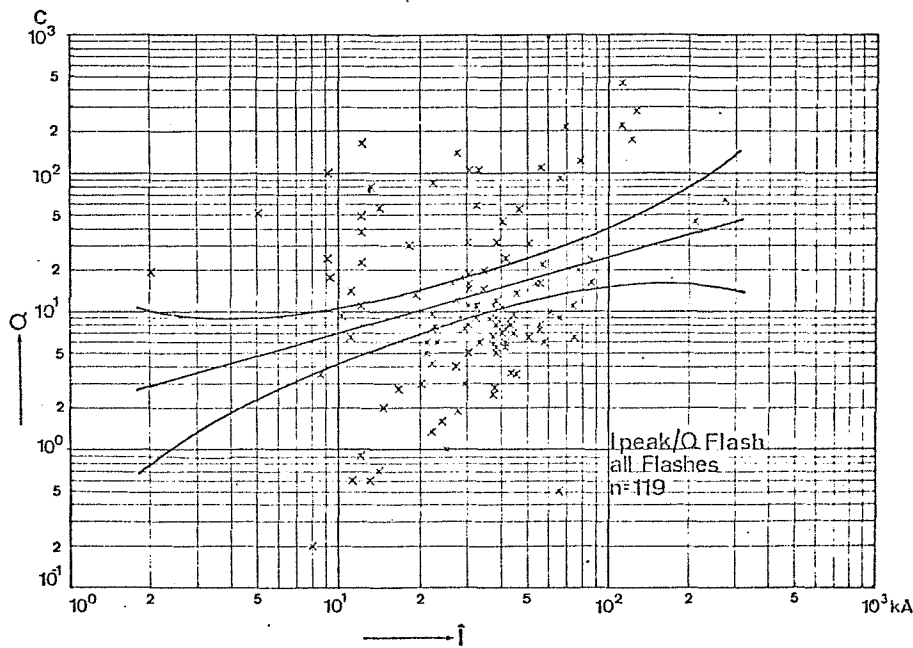
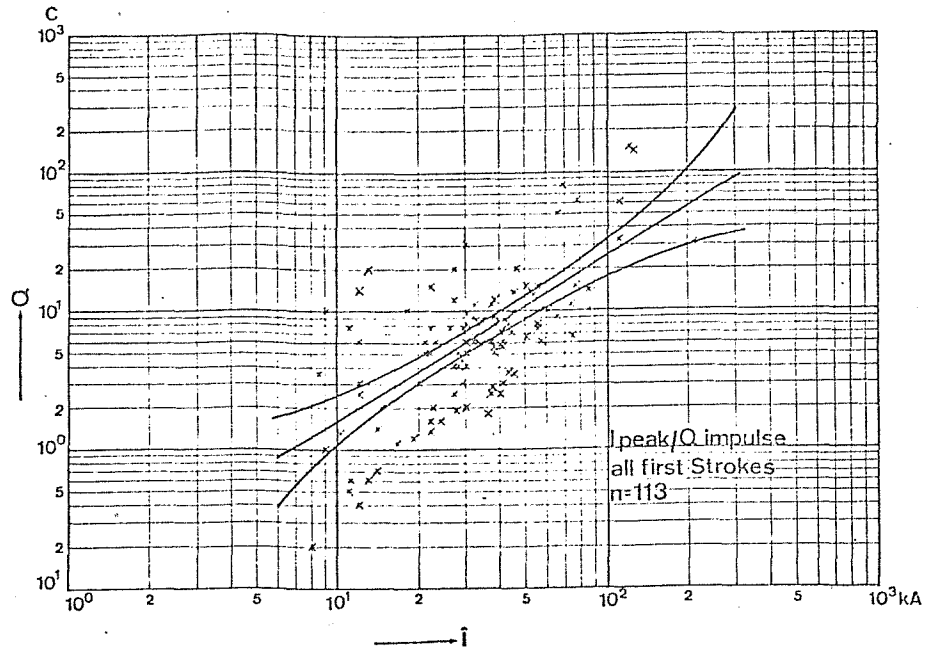


Fig. 28  
Korrelation zwischen Scheitelwert  $i$  und  
Ladung  $Q$  für Gesamtblitze  
 $n$  Anzahl Messungen

Fig. 29  
Amplitudenspektrum des Blitzstromes gemäss  
Oszillogrammen No 63072 und 70062  
 $n$  Anzahl Messungen

